DNA 4859F

TECHNOLOGY STUDY ON PIEZOELECTRIC MATERIALS

W.B. Harrison
A.G. Thalheimer
Honeywell, Inc.
Avionics Division
P.O. Box 11563
St. Petersburg, Florida 33733

20 July 1979

Final Report for Period July 1978—December 1978

CONTRACT No. DNA 001-78-C-0328

THIS WORK SPONSORED BY THE DEFENSE NUCLEAR AGENCY
UNDER RDT&E RMSS CODE B323078464 Z99QAXTD40106 H2590D.

Prepared for
Director
DEFENSE NUCLEAR AGENCY
Washington, D. C. 20305

Destroy this report when it is no longer needed. Do not return to sender.

PLEASE NOTIFY THE DEFENSE NUCLEAR AGENCY, ATTN: STTI, WASHINGTON, D.C. 20305, IF YOUR ADDRESS IS INCORRECT, IF YOU WISH TO BE DELETED FROM THE DISTRIBUTION LIST, OR IF THE ADDRESSEE IS NO LONGER EMPLOYED BY YOUR ORGANIZATION.

(18) DNA, SBIE

UNCLASSIFIED

SECURITY CLASSIFICATION OF THIS PAGE *(When Data Entered)*

(19) **REPORT DOCUMENTATION PAGE**

READ INSTRUCTIONS BEFORE COMPLETING FORM

1. REPORT NUMBER: DNA 4859F — AD-E300 644
2. GOVT ACCESSION NO.
3. RECIPIENT'S CATALOG NUMBER

4. TITLE (and Subtitle): TECHNOLOGY STUDY ON PIEZOELECTRIC MATERIALS (6)

5. TYPE OF REPORT & PERIOD COVERED (9): Final Report, For Period Jul [illegible]–December [illegible]78
6. PERFORMING ORG. REPORT NUMBER: 1

7. AUTHOR(s) (10): W. B. Harrison, A. G. Thalheimer
8. CONTRACT OR GRANT NUMBER(s) (15): DNA 001-78-C-0328

9. PERFORMING ORGANIZATION NAME AND ADDRESS: Honeywell, Inc., Avionics Division, P.O. Box 11563, St. Petersburg, Florida 33733
10. PROGRAM ELEMENT, PROJECT, TASK AREA & WORK UNIT NUMBERS (12): Subtask Z99QAXTD401-06

11. CONTROLLING OFFICE NAME AND ADDRESS: Director, Defense Nuclear Agency, Washington, D.C. 20305
12. REPORT DATE (11): 20 Jul [illegible]79
13. NUMBER OF PAGES: 56

14. MONITORING AGENCY NAME & ADDRESS *(if different from Controlling Office)* (13) 38
15. SECURITY CLASS *(of this report)*: UNCLASSIFIED (17) D 40 7
15a. DECLASSIFICATION/DOWNGRADING SCHEDULE

16. DISTRIBUTION STATEMENT *(of this Report)*

Approved for public release; distribution unlimited.

17. DISTRIBUTION STATEMENT *(of the abstract entered in Block 20, if different from Report)*

18. SUPPLEMENTARY NOTES

This work sponsored by the Defense Nuclear Agency under RDT&E RMSS Code B323078464 Z99QAXTD40106 H2590D.

19. KEY WORDS *(Continue on reverse side if necessary and identify by block number)*

Low Z Materials
Piezoelectrics
Micropositioning
Laser Gyros
Path Length Control
Radiation Stability

20. ABSTRACT *(Continue on reverse side if necessary and identify by block number)*

The use of Honeywell's ring laser gyros technology is being considered for maneuvering reentry vehicle guidance where hostile nuclear radiation environments may be encountered by the ring laser gyro and its path length control (PLC) transducer. In an effort jointly sponsored by SAMSO and DNA, Honeywell and IRT[1] performed tests and analytical analysis on an operating laser gyro. It was shown that some "mode hopping" transient motions were produced by the PLC transducer when subject to x-ray exposure. The materials

(IRT 1)

DD FORM 1 JAN 73 1473 EDITION OF 1 NOV 65 IS OBSOLETE

UNCLASSIFIED

SECURITY CLASSIFICATION OF THIS PAGE *(When Data Entered)*

292 915

20. ABSTRACT (Continued)

used in the PLC transducer were analyzed and the high Z lead zirconate-lead titanate (PZ-PT) materials used in the transducer were considered as a partial cause of this phenomena. This program was therefore initiated to determine if lower Z materials, free of lead, were suitable replacements for the PZ-PT used in the PLC driver section of the transducer.

PREFACE

This contract funded by the Defense Nuclear Agency covers the technical effort performed before 26 June 1978 through 31 December 1978 to investigate techniques to improve the radiation resistance and stability of the piezoelectric actuators used for mirrors in laser gyros and similar devices. This effort primarily considers nonlead piezoelectric on electrostrictive materials which could replace the currently used lead zirconate-lead titanate ceramic.

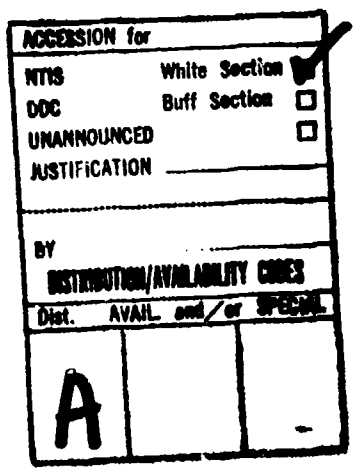

TABLE OF CONTENTS

LIST OF ILLUSTRATIONS

LIST OF TABLES

SECTION 1
INTRODUCTION

BACKGROUND

The typical Honeywell ring laser gyro is built, as shown in Figure 1, from a very low thermal expansion, fused silica type material CERVIT which is used for the primary block. The primary function of the block is to provide a high quality gas container and an ultrastable aperture and mounting surfaces for the various mirrors, anodes and cathodes attached to the block. The anodes and cathodes of course initiate and maintain the two helium-neon laser beams traveling in opposite directions. Two stationary and one movable mirror are used to provide an active closed-loop path length control system to maintain a constant operating point for the gyro. The control loop functions so that the gyro output power, monitored by one of the photoconductive detectors, is continuously maximized. Changes in the gyro path length result in variations in gyro power output and scale factor. The relationship between gyro scale factor, power output and path length are shown in Figures 2 and 3. The variations in scale factor are repetitive from mode to mode; however, there is an absolute shift in scale factor of approximately three parts per million per mode.

The moveable mirror or path length control (PLC) transducer is typically designed as shown in Figure 4. The three main components of the PLC transducer are: the fused silica (CERVIT) transducer with its movable mirror surface held in place by the thick CERVIT diaphram; the driver section which is composed of two discs of PZ-PT mounted on a CERVIT plate; and an Invar mounting nut and bolt to hold the driver to the mirror section. As the voltage applied to the driver is increased or decreased the driver deflects and forces the mirror forward or backward respectively.

PLC TRANSDUCER STABILITY TO X-RAYS

Three primary areas of concern, identified in an earlier investigation[1], relate to the PLC transducer. These are 1) the path length changes caused by x-ray

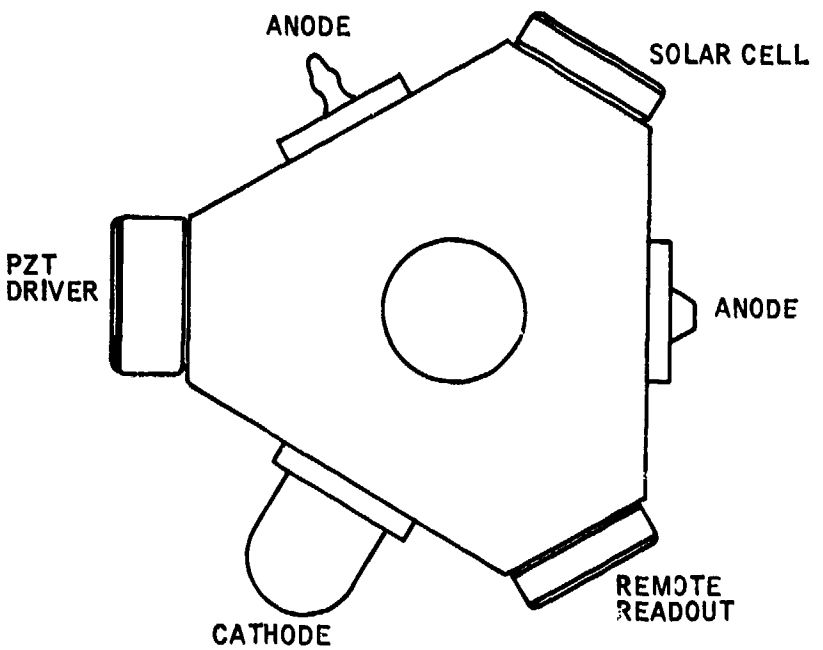

Figure 1. Laser gyro block assembly.

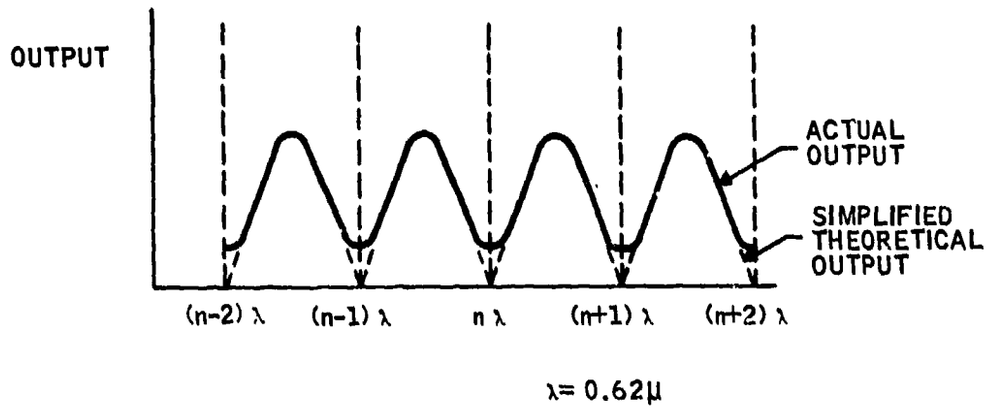

Figure 2. Laser gyro output versus path length.

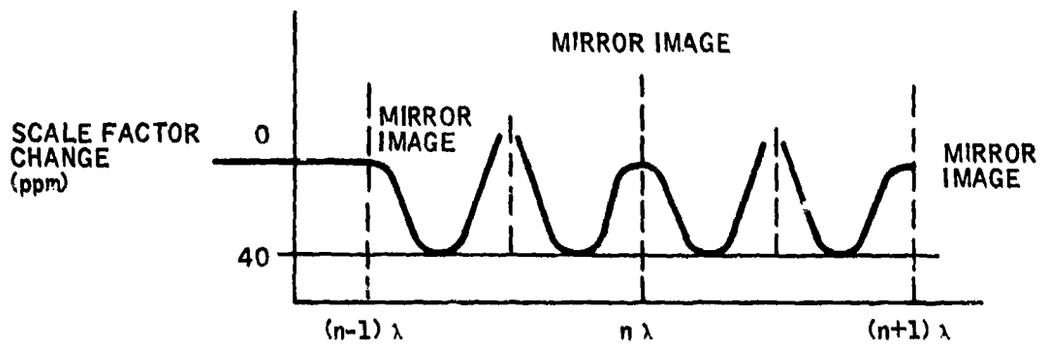

Figure 3. Laser gyro scale factor versus path length.

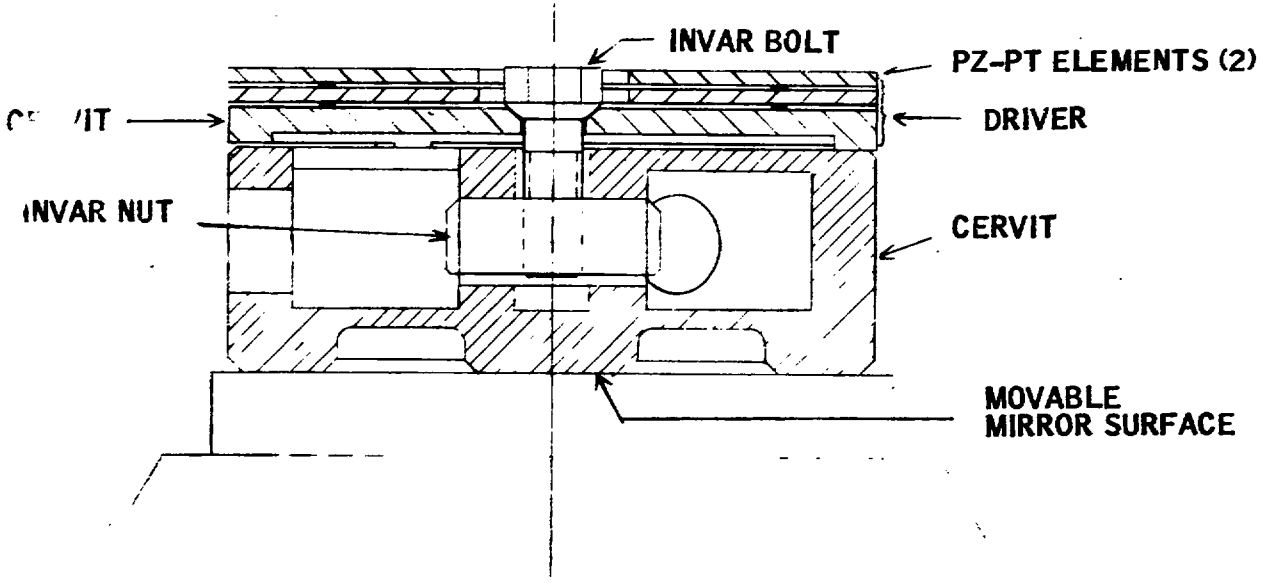

Figure 4. PLC transducer - present configuration.

heating of the PLC transducer assembly, 2) the recovery time of the PLC subsystem from high intensity x-radiation and 3) the potential for unidentifiable mode changes caused by x-ray heating.

The first response of the PLC transducer assembly to the nearly instantaneous temperature rise produced by x-ray exposure is a discrete spectrum of millisecond type mechanical oscillations as illustrated in Figure 5. The primary source of these oscillations is the PZ-PT driver element excited by energy disposition from x-rays. The PLC transducer assembly also produces a long term transient path length change lasting for many seconds as in Figure 5. The initial magnitude of the transient may exceed one wavelength (λ). The time duration of this transient is determined by the equilibration characteristics of the transducer and cooling provided.

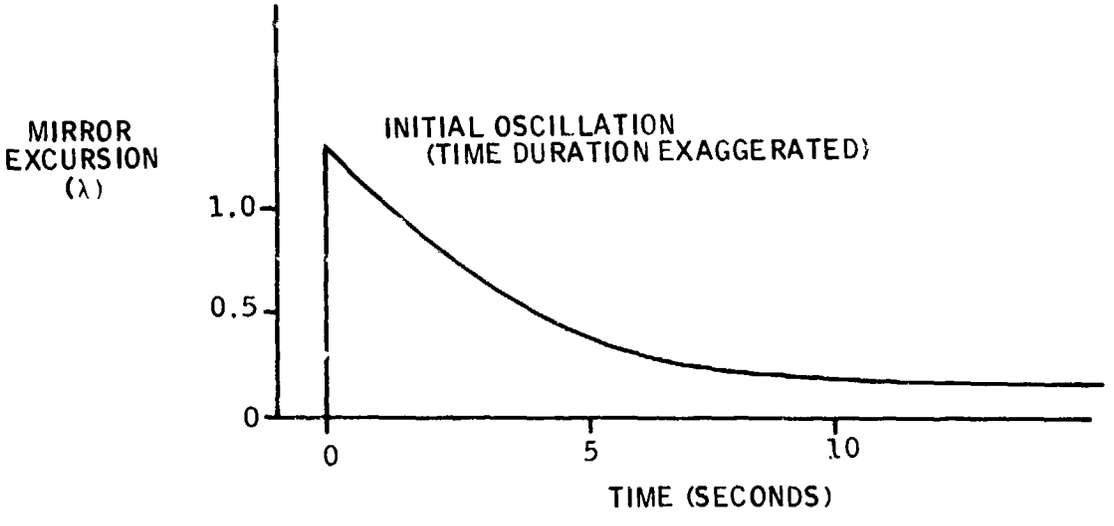

Figure 5. Path length transducer x-ray response.

When the PLC transducer senses short term radiation induced transients, which are greater than a half wavelength, the subsystem may lock the gyro into an undefined operating mode and errors in scale factor may exceed six parts per million. Long term transient charges of 30 seconds were shown to produce small angular (0.1°) roll errors; however, these are well within the error budget and the recovery time of the PLC subsystem was found to sufficiently quick to maintain angular error buildup within bounds. It was therefore concluded that the errors in scale factor should be brought under control.

The most effective means of correcting this problem would be to redesign the PLC transducer to reduced the average atomic mass (Z) of the materials used in the construction of the driver.

SECTION 2
EXPERIMENTAL EFFORT

This section presents the experimental approach, discussion and results of the experimental effort on this program to define lower molecular weight materials for the PLC driver and to arrive at a more stable transducer design for using these materials.

APPROACH

The objective of this study on "Non-Leaded Piezoelectric Materials" is to improve the radiation resistance stability of the piezoelectric drivers used on the path length control PLC transducer for laser gyros. The initial task was a literature search and material selection to identify low atomic number (Z) non-lead containing piezoelectric or electrostrictive materials for further study. The materials identified were then evaluated at high voltages to determine their electric field versus displacement characteristics. Based on the activity obtained, several materials and conceptual designs for PLC drivers and transducers were examined for a follow-on study program.

LITERATURE SEARCH

Five primary sources of literature were reviewed for articles on ferroelectric and dielectric materials with high electromechanical displacements. These included 1) International Aerospace Abstracts, 2) U.S. Government Research and Development Reports, 3) Ceramic Abstracts, 4) Ferroelectrics and 5) books devoted to ferroelectric materials.

Ferroelectrics, an international journal, contains two continuously updated bibliographies, one by Lang, "Literature Guide to Pyroelectricity" and the other by Toyoda, "Bibliography of Ferroelectrics." Toyoda gives a listing of articles, books and conference proceedings dealing with ferroelectrics and related materials published throughout the world. About 9000 listings for the last six years were

reviewed for new materials which did not contain lead or other elements with an atomic number greater than 56 (Barium) as a primary constituent.

The materials found, which had sufficient data reported to determine their electromechanical behavior, are given in Table 1 according to their average atomic mass and compared to the $PbZrO_3$ - $PbTiO_3$ presently used in the PLC transducer. These 35 materials can be broken down into five classes: 1) perovskite-type oxides, 2) aqueous solution grown crystals, 3) semiconductive compounds, 4) other oxides and 5) organic polymeric compounds.

In order to avoid confusing molecular mass with atomic mass, consider TGS. The molecular mass of this chemical compound is large, even though it is composed of a large number of light elements. Triglycine Sulfate (TGS) $(NH_3\ CH\ OOH)_3\ SO_4$, which has a 32 atom molecule for a molecular mass of 321, has an average atomic mass (per atom) of only 10. In x-ray vulnerability considerations, it is desirable to reduce the temperature rise with its commensurate thermal distortion. There are two ways to do this: 1) select a low atomic number (Z) material, because for a given x-ray dose different atoms extract energy about as Z^4; or 2) select a material with a high heat capacity to minimize the temperature rise associated with the deposition of x-ray energy. In essence, the room temperature heat capacity of most materials is described by the equipartition theorem, also called the law of Dulong and Petit. This rule says that the internal energy of any atom in a solid is proportional to is 3 kT, where k is the Boltzmann's constant, so the heat capacity of a mole of atoms is 3 rN kT which is also 3 rR (per mole) where r is the number of atoms per molecule, and R is the universal gas constant (1.98 cal/mole°). This means for example, that although water (H_2O) and Sodium (Na) have very similar molecular masses (18 vs. 19) and hence will extract nearly equal amounts of energy per molecule from a given x-ray, they will not heat equal amounts. Water, which has 3 atoms per molecule, will have a heat capacity of about 16 cal/mole °C = 1 cal/gm °C ≃ 0.3 cal/gm-°C. Since water's heat capacity is three times that of sodium, sodium would be heated three times as much as water by identical x-rays. [24]

Perovskite-Type Oxides

Sixteen of the materials in Table 1 have the general formula ABO_3 which normally have a distorted perovskite, simple cubic structure. The A-type cation at the

Table 1. Piezoelectric properties of materials. (sheet 1 of 2)

Form	Material	Mol. Weight	Average Atomic Mass	Curie Temp. (°C)	Density gm/cc	Dielectric Constant	Piezoelectric				Reference
							Coupling	Strain Constant m/v (10^{-12})	Voltage Constant V/M (10^{-3})	Compliance $m^2/N(10^{-12})$	
S.C.	$(NH_3)h_2PO_4$ (ADP) (0° Z-Cut)	99	9	125	1.80	32	0.32	48	354	53	2, 3
S.C.	$(NH_3CH\ OOH)_3SO_4$ TGS	321	10	46							4
S.C.	$NaKC_4H_4O_6 \cdot 4H_2O$ (45° X-Cut)	282	10	45	1.77	350	0.78	275	98	57	3
S.C.	(Rochelle Salt) (45° Y-Cut)	282	10	45	1.77	10	0.29	29	290	99	3
Organic	$(CH_2CH_2)_n$ Polyvinylidene	$(64)_n$	11	110	1.8	11	0.16	14	140		5, 6
S.C.	BeO	25	13		3.01	8	0.02	0.2		3	7
S.C.	$Li_2SO_4\ H_2O$(LH) (0°Y-Cut)	128	13	100	2.06	10	0.38	16	175	20	2, 8
S.C.	$K\ H_2\ PO_4$ (KDP) (0° Z-Cut)	136	17	150	2.34	21	0.12	21	102	49	2, 3
S.C.	$H_4NaMn_3Al_5B_3Si_6O_{31}$ (Tourmaline)	1050	19		3.10	1700	0.10	2			3, 9
S.C.	Quartz (SiO_8) (Y-Cut)	60	20	550	2.65	5	0.10	2	58	12	3
S.C.	AlN	41	21		3.26	9	0.20	6	61	2.8	8
S.C.	RbH_2PO_4 (RbDP)	183	23		2.8	248		3		23	10
S.C.	$LiGaO_2$	109	27		4.19	9	0.25	8	93		3
S.C.	$Li\ NbO_3$	148	30	1210	4.70	30	0.16	6	23	5.0	8
S.C.	$K_3Li_2Nb_5O_{15}$	836	33	420		120	0.64				11
Ceramic	$Na_{0.8}Cd_{0.1}NbO_3$	171	34	240		2000	0.42	200	11		1

Table 1. Piezoelectric properties of materials. (sheet 2 of 2)

Form	Material	Mol. Weight	Average Atomic Mass	Curie Temp. (°C)	Density gm/cc	Dielectric Constant	Coupling	Strain Constant m/v (10^{-12})	Voltage Constant V/M (10^{-3})	Compliance m^2/N (10^{-12})	Reference
Ceramic	$Na_{0.5}K_{0.5}NbO_3$	172	34	420	4.46	496	0.46	127	29	10	12, 13
S.C.	$LiIO_3$	132	36	256	4.47	6	0.51				14
S.C.	$Sr_4K\ LiNb_{10}O_{30}$	1806	39			870	0.48				15
S.C.	ZnO	81	41		5.68	11	0.41	11	109	6.9	8, 16
S.C.	$K_3Li_2(Ta_{0.46}Nb_{0.54})_5O_{15}$	1038	42	160		360	0.50				11
S.C.	$Ba_2NaNb_5O_{15}$	1002	44		5.3	51	0.57	37	82	8.3	17
S.C.	$(Sr_{0.5}Ba_{0.5})Nb_2O_6$	396	44	120		400	0.54	- 20			16, 18
Ceramic	$BaTiO_3/CaTiO_3$ 95/5	228	46	120	5.50	1100	0.45	140	14	9.1	19
Ceramic	$BaTiO_3/CaTiO_3/PbTiO_3$ 85/7.5/7.5	231	46	145	5.25	600	0.30	100	19	9.4	19
Ceramic	$BaTiO_3/ZrO_3$ 98/2	231	46	103		1075		- 70	8		1
S.C.	$BaTiO_3$	233	46	120	5.7	1900	0.49	191	11		1, 12
S.C.	$LiTaO_3$	236	47	630	4.19	45	0.18	8	21	4.4	8, 20, 16
S.C.	ZnS	97	49		4.09	8	0.08	2			8
S.C.	$SrTeO_3$	263	53		4.32	97	0.34	42	282	23	21
S.C.	$KTaO_3$	265	53	-260							
Ceramic	$Pb_{0.94}Sr_{0.06}(Zr_{0.53}Ti_{0.47})O_3$ (PZ-PT)	326	65	300	7.6	1250	0.65	230	25	15	19
S.C.	CdS	144	72		4.82	92	0.26	10	113	21	22
S.C.	GaAs	145	73		5.31	11	0.07	3		1.2	23
S.C.	CdSe	191	86		5.67	11	0.19	8	83	17	2, 16
S.C.	ZnTe	193	87		5.64	10	0.02	0.5			8
S.C.	SbSI	281	94	20		2200	0.87				8

corners of a cube is coordinated with twelve oxygen ions at the center of each face and the B-type cation at the body center is coordinated with six oxygen ions. These can also be subdivided into three groups according to the valence state of the A and B-site elements such as $A^{+1}\ B^{+5}O_3$, $A^{+2}B^{+4}O_3$ and complex mix valence state of these sites. The ferroelectric compounds formed normally have rhombohedral, tetragonal or orthorhombic symmetry. In the following discussion we will discuss the materials according to their valence state and not their crystallographic state. Indeed, some of the materials ($LiNbO_3$ and $LiTaO_3$) do not have the perovskite-type structure. The first group are seven $A^{+1}B^{+5}O_3$ materials which include $LiNbO_3$, $(Na_{0.5}K_{0.5})\ NbO_3$, $LiTaO_3$, $KTaO_3$, $K_3Li_2Nb_5O_{15}$, $LiIO_3$ and $K_3Li_2(Ta_{0.46}\ Nb_{0.54})_5O_{15}$. The ceramic form of sodium potassium niobate has good piezoelectric properties, a high Curie temperature and about half the average atomic mass as the presently used PZ-PT. Lithium niobate has been used extensively as a single crystal because of its very high Curie temperature (1210°C) and its acoustic surface wave properties. Large single crystals are readily available but have a fairly high price and poor piezoelectric properties. The other five materials either have poor piezoelectric properties or insufficient information was available at this time to judge the suitability of their properties for the PLC displacement transducer.

Six $A^{+2}B^{+4}O_3$ compounds were identified which included four types of $BaTiO_3$, $(Sr_{0.5}Ba_{0.5})\ Nb_2O_6$ and $SrTeO_3$ as well as the presently used PZ-PT. Two of the barium titanate ceramic materials have been used extensively as piezoelectric ceramics, predating PZ-PT by about ten years. Two of the $BaTiO_3$ modifications contain $CaTiO_3$ or $CaTiO_3$ and $PbTiO_3$ and are produced at Honeywell as Type 101 and 113 $BaTiO_3$, respectively. Both have good piezoelectric behavior and were used as displacement transducers prior to the discovery of the more active PZ-PT in other devices (not the laser gyro). Their average atomic mass is about 30 percent less than PZ-PT, but they have a low Curie temperature. Single crystal $BaTiO_3$ has better properties but is difficult and not practical to produce in large shapes. The other two materials offer no advantage in piezoelectric properties and have higher molecular weights.

Three complex ABO_3 materials, where compensating valencies are used to achieve either $A^{+1}B^{+5}O_3$ or $A^{+2}B^{+4}O_3$ compounds, were identified as $(Na_{0.8}Cd_{0.1})\ NbO_3$, $Ba_2Na\ Nb_5O_{15}$ and $Sr_4\ K\ Li\ Nb_{10}O_{30}$. While the last two of these contain lighter elements, their average atomic mass was sufficiently high to rule them out as candidate PLC materials. The $Na_{0.8}Cd_{0.1}NbO_3$ ceramic material is of interest

because it does have a high Curie temperature and good piezoelectric properties. In fact, its strain constant is second best to all of the materials considered as a substitute for the PZ-PT currently used. This material is not now currently commercially produced and a production process would have to be developed before this material could be applied to displacement transducers.

Aqueous Solution Growth Crystals

Six of the materials described in Table 1 were derived by the aqueous solution growth of single crystals. These were attractive because their average atomic mass was about 80 percent less than PZ-PT. They include ammonium dihydrogen phosphate (ADP), potassium dihydrogen phosphate (KDP), Rubidium dihydrogen phosphate (RDP), sodium potassium tartarate (Rochelle salt), triglycine sulfate (TGS), and lithium sulphate (LH). Rochelle salt had the highest piezoelectric constants and has been used extensively in various older transducer designs, however, it has two primary drawbacks. Its Curie temperature is only 45°C and its piezoelectric output is very water sensitive. The strain constant for those crystals, which are 45° x-cut, are found to be better than $(Na_{0.8}Cd_{0.1})\ NbO_3$ reported above and almost equal to PZ-PT. TGS and Rochelle salt have average atomic mass about one third that of sodium cadmium niobate reported above. The other materials, while much lower in molecular weight, have relatively poor piezoelectric strain constants. TGS also contained no elements with an atomic number greater than 16 (Sulfur).

Semiconducting Compounds

Eight semiconducting compounds are cited in Table 1, AlN, ZnO, ZnS, CdS, GaAs, CdSe, ZnTe and SbSI. All of these have a lower molecular weight than PZ-PT. For instance, the average atomic mass varied from 21 for AlN to 94 for SbSI as opposed to 65 for PZ-PT. The piezoelectric strain constants of these materials are less than 5 percent of that produced by PZ-PT even though SbSI had a high coupling coefficient of 0.67.

Other Oxides

Four other oxides, including quartz, probably the most widely used transducer material, were listed in Table 1. In addition to quartz, BeO, $LiGaO_2$ and Tourmaline, a complex silicate, were included. Tourmaline (like quartz) is a naturally occuring crystal which was one of the first piezoelectric materials identified. Again, while these contain low molecular weight elements, they have very weak piezoelectric strain constants.

Polymeric Compounds

Recently, (18, 19) the piezoelectric behavior of several polymeric materials have been studied and found to exhibit significant piezoelectric properties. One of the more promising materials identified is polyvinylidene fluoride (PVF_2) which is $(CH_2 + CF_2)n$. The properties of this material are also given in Table 1. Even though this material has been shown to be quite useful as a mechanical to electrical hydrophone type transducer material, it has very poor ability to convert electrical energy into mechanical motion as necessary for the PLC transducer.

PROCEDURES

Ten of the 35 materials discussed above were selected for further test, evaluated and then compared to the present PZ-PT used. Those selected, and their class, are included in Table 2. None of the polymeric and semiconducting type materials were selected for further study because of their low piezoelectric strain constants. The first three materials selected are ceramic type materials which are standard materials produced at Honeywell. The $(Sr_{0.5}Ba_{0.5})Nb_5O_{15}$ and K Ta O_3 single crystal materials were grown by Liu (9, 15) at our Corporate Materials Science Center. The TGS and $LiGaO_2$ were obtained from Phillips Research and the Rochelle salt and $LiNbO_3$ were produced by Clevite and Crystal Technology, respectively. The $(Na_{0.8}Cd_{0.1})$ NbO_3 and $(Na_{0.5}K_{0.5})$ NbO_3 are ceramic materials which require a detailed compositional development effort; therefore, samples of these were not available for further testing.

Table 2. Experimental Materials

Material	Average Atomic Mass	Source	Class and Form					Shape		
			Perovskite			Aqueous Solution Grown	Other Oxide	"Z" Axis	"X" Axis	"Y" Axis
			$A^{+1}B^{+5}O_3$	$A^{+2}B^{+4}O_3$	Complex					
Hot Pressed K-13 PZ-PT	65	Honeywell		C				0.400	0.180	0.180
$BaTiO_3/CaTiO_3$ Type 101	46	Honeywell		C				0.400		
$BaTiO_3/CaTiO_3/PbTiO_3$ Type 113	46	Honeywell		C				0.400		
$(Sr_{0.5}Ba_{0.5})Nb_5O_{15}$	44	Honeywell		S.C.				0.400	0.165	0.127
$LiNbO_3$	30	Crystal Tech	S.C.					0.223	0.195	0.539
$(Na_{0.5}K_{0.5})NbO_3$	34	*	C						*	
$KTaO_3$	53		S.C.					0.200	0.200	0.250
$(Na_{0.8}Cd_{0.1})NbO_3$	34	*			C				*	
Rochelle Salt	10	Clevite				S.C.		0.631	0.431	0.319
TGS	10	Phillips				S.C.		0.225	0.295	0.454
$LiGaO_2$	27	Phillips					S.C.	0.245	0.220	0.396

C - Ferroelectric Polycrystalline Ceramic

SC - Single Crystal

* - Not commercially available

One to eight samples of eight of the materials given above were prepared into field versus displacement test specimens. Each sample was shaped to the size indicated in Table 2 by diamond sawing and grinding. The long dimension (z-axis) of all samples was the growth or initial poling direction of all materials. Fired silver electrodes were applied to the PZ-PT and $BaTiO_3$ samples prior to poling each material at about 60 volts/mil at 145° and 140°C, respectively. Conductive epoxy-silver or aluminum foil electrodes were used on the other materials when the field was applied in the transverse, d_{15} direction. Side electrodes were applied and leads were attached after removing the top and bottom polarization electrodes.

The first application of d.c. voltage was applied in the same direction as the poling field while the displacement was measured as shown in Figure 6. A positive voltage of at least 37.5 volts/mil was applied, reversed to zero and then to a negative voltage to obtain the depoling switching voltage. Five positive voltage cycles were then applied from 0 to +37.5 volts/mil to stabilize the displacement. The percent extension was measured at 35 volts/mil, the "d" constant was calculated for this field and then reported in Table 3.

The high voltage power supply had an automatic triangle ramp where the full cycle with change of polarity takes one minute. An automatic half cycle with no change of polarity could also be run. The peak voltage could also be set prior to the automatic cycle. To calibrate the unit, a dial indicator, the transducer amplifier, and the x position of the recorder pen were zeroed. Voltage on the ceramic was raised manually to give a dial indicator deflection of 0.0005 inch . Sensitivity of transducer amplifier and x- calibration of recorder were adjusted to give a known travel to the recorder pen. Most studies were run with a sensitivity of 20 cm = 0.0005 inch.

Automatic cycles were normally run without the dial indicator because its pressure was found in some cases to influence the shape of the loop. The sample was then only under the dead weight of the plexiglas rod (about 90 gm) plus whatever pressure was exerted by the transducer probe.

Data obtained in this manner is similar to d_{33} where the extension is measured in the same direction as the voltage. A second set of data was then determined where the voltage was applied to the length of the sample and extension was measured perpendicular to the poling direction (d_{31}). The end electrodes were removed and air cured electrodes were applied on two sides perpendicular to the original poling

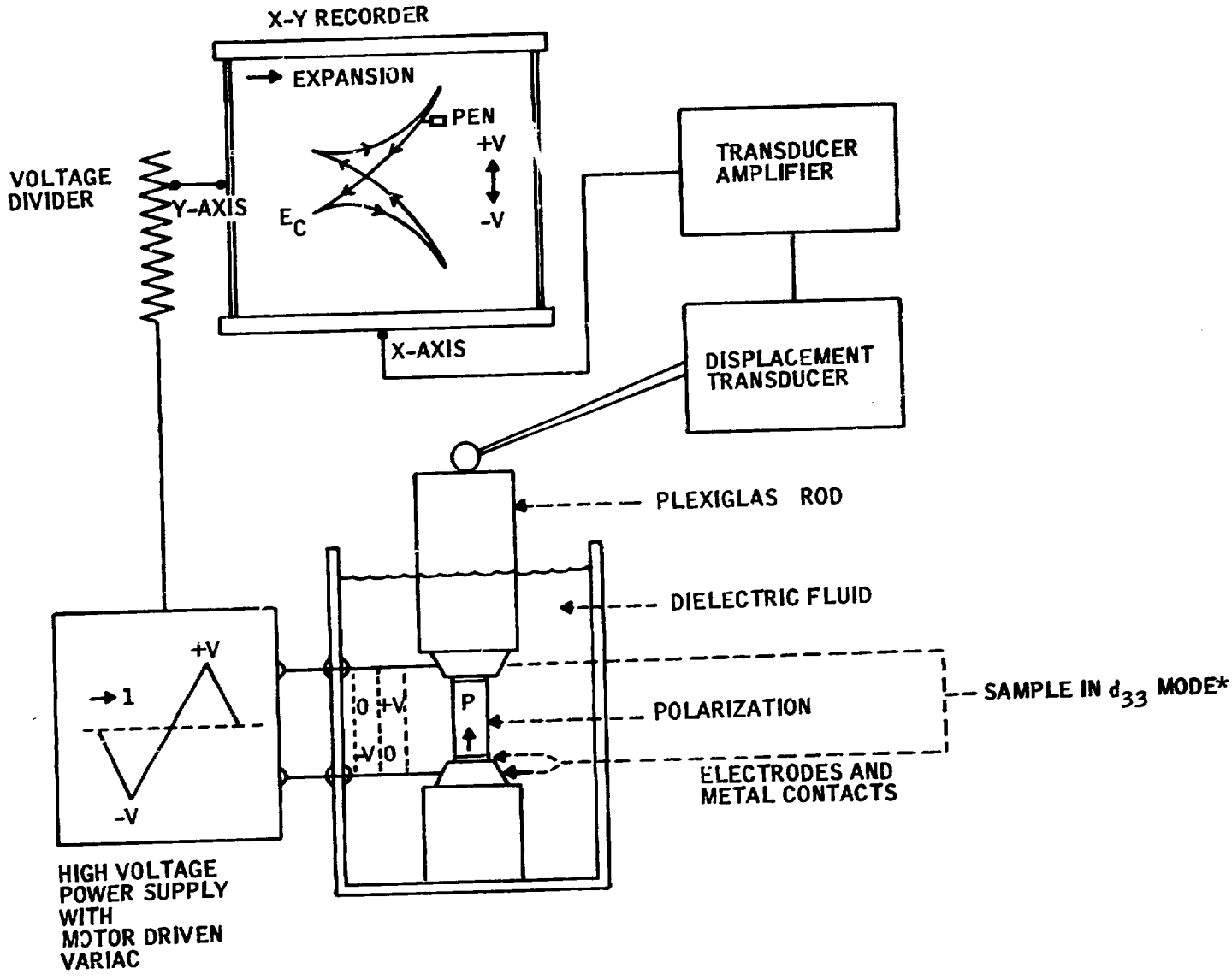

Figure 6. Field versus extension test apparatus.

Table 3. High voltage strain constants for experimental material.

Material	Average Atomic Mass	Field V/mil	d_{33} m/v(10^{-12})	d_{31} m/v(10^{-12})	d_{15} m/v(10^{-12})
Hot Pressed K-13 PZ-PT	65	35	+428	-219	-125
Type 101 $BaTiO_3$	46	35	+228	-85	-76
Type 113 $BaTiO_3$	46	35	+134	-47	-24
Rochelle Salt	10	35 35	-48 +24	+147 -4	
TGS	10	133		-30	
$(Sr_{0.5}Ba_{0.5})Nb_5O_{15}$	44	35	+81		
$LiNbO_3$	30	35 76	+23 +51		
$LiGaO_2$	27	35 87	-4 -9		
$LiTaO_3$	53	35 100	+1 +12		

direction, voltage was applied and extension was measured in the original polarization direction (d_{15}). The electrode set up is shown in the inset of Figure 7.

RESULTS AND DISCUSSION

Figures 8 to 13 show the typical field versus extension plots for the experimental materials evaluated in this program. Figure 8 shows the full loop behavior of the presently used Honeywell hot-pressed K-13 PZ-PT and two possible substitutes, type 101 and 113 $BaTiO_3$. These show the percent extension in thickness of a part (d_{33}-mode) where voltage is initially applied across the thickness in the same direction as the original polarization field and then reversed to reach a negative field which tends to reverse polarization. The resistance to depolarization depends upon the type of doping. The K-13 PZ-PT (acceptor doped with strontium) exhibited very slight switching or depolarization at 35 volts/mil wheras the type 113 and 101 $BaTiO_3$ started to switch at 22 and 12 volts/mil, respectively. The type 113 $BaTiO_3$ (doped with $CaTiO_3$ and $PbTiO_3$) is compounded to have greater field stability but has a lower percent extension than the type 101 $BaTiO_3$. In normal operation positive voltages can be used up to about 80 volts/mil or the breakdown limit of the material and to a negative field which is about 75 percent of the switching field given above. Figures 9 and 10 show half loops for three operational modes--d_{33}, d_{31} and d_{15}. These data are also summarized in Table 3 for a comparable field of 35 volts/mil. Note that while the Type 101 $BaTiO_3$ has almost twice the output of the type 113 $BaTiO_3$, the latter material has lower hysteresis and a higher switching field and thus higher stability.

The six other experimental materials evaluated are shown in Figures 10 to 12; most of these had significantly less field versus strain capability as compared to the $BaTiO_3$.

Rochelle salt as shown in Figure 11 does show a very high d_{31} strain (157×10^{-12} M/V) which would be desirable for a disc type PLC transducer and the average atomic mass was 75 percent less than $BaTiO_3$, but is quite moisture sensitive. Also the hydroxyl ions in this material are expected to make it quite sensitive to radiation degradation.[25] As shown in Figure 12, Triglycine sulfate had a threshold field of about 40 volts/mil which had to be exceeded before any appreciable

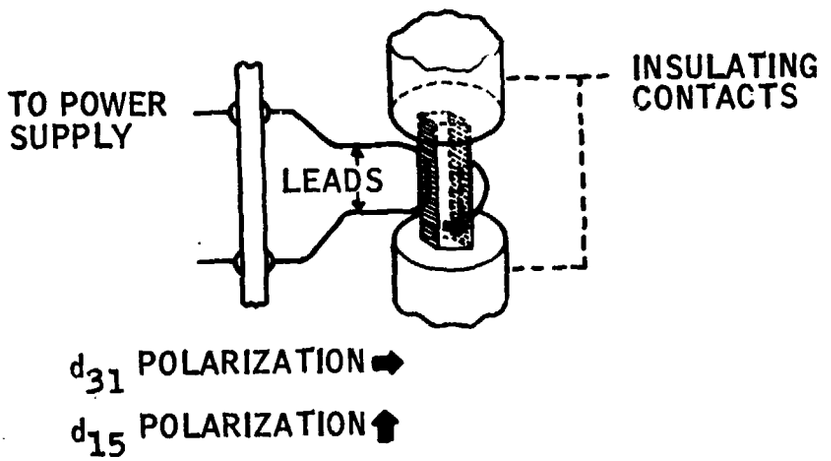

Figure 7. Set-up transverse (d_{31}) or shear (d_{15}) modes.

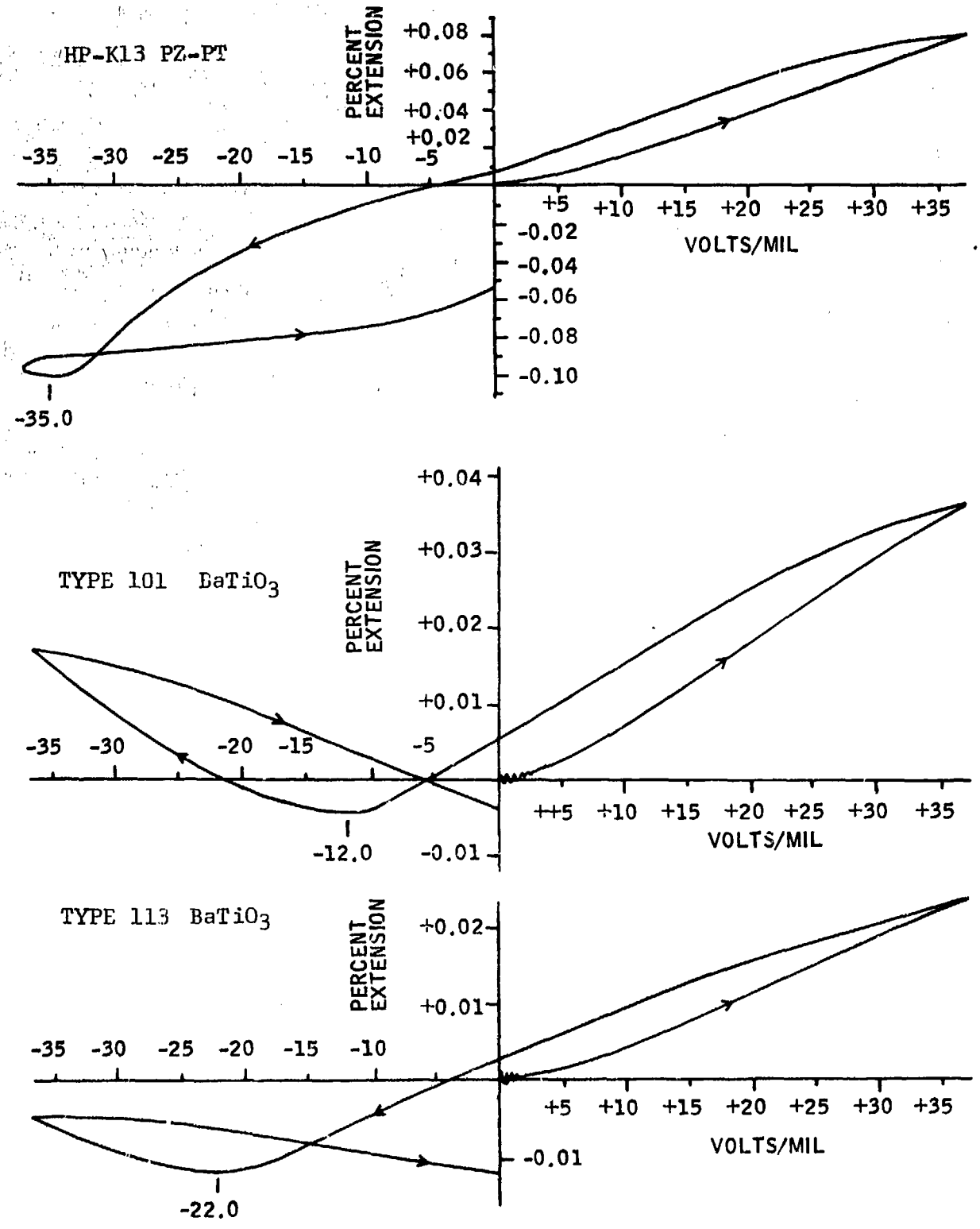

Figure 8. Field versus extension PZ-PT and $BaTiO_3$ 33 mode.

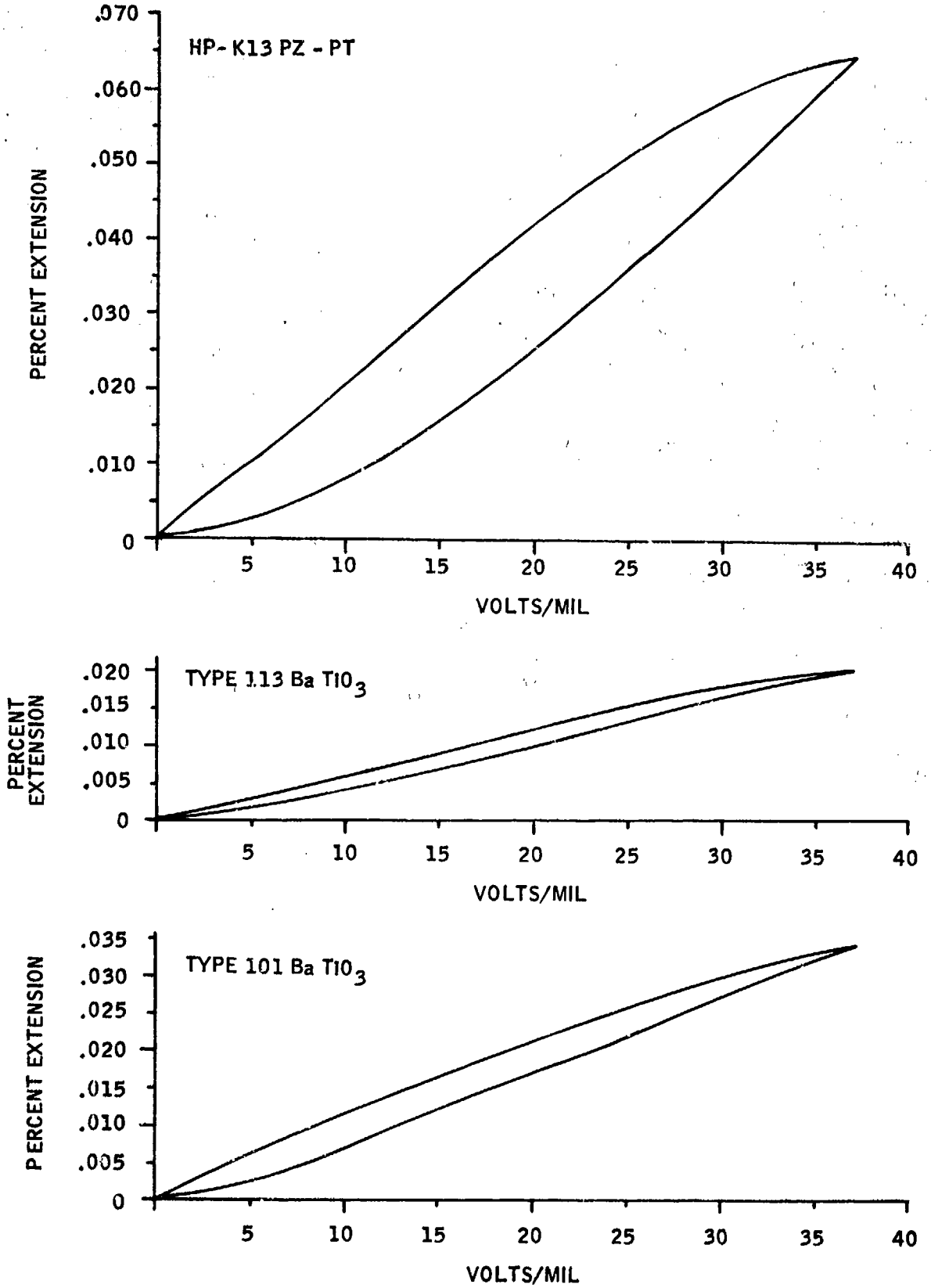

Figure 9. Field versus extension (half loop) poled material d_{33} mode.

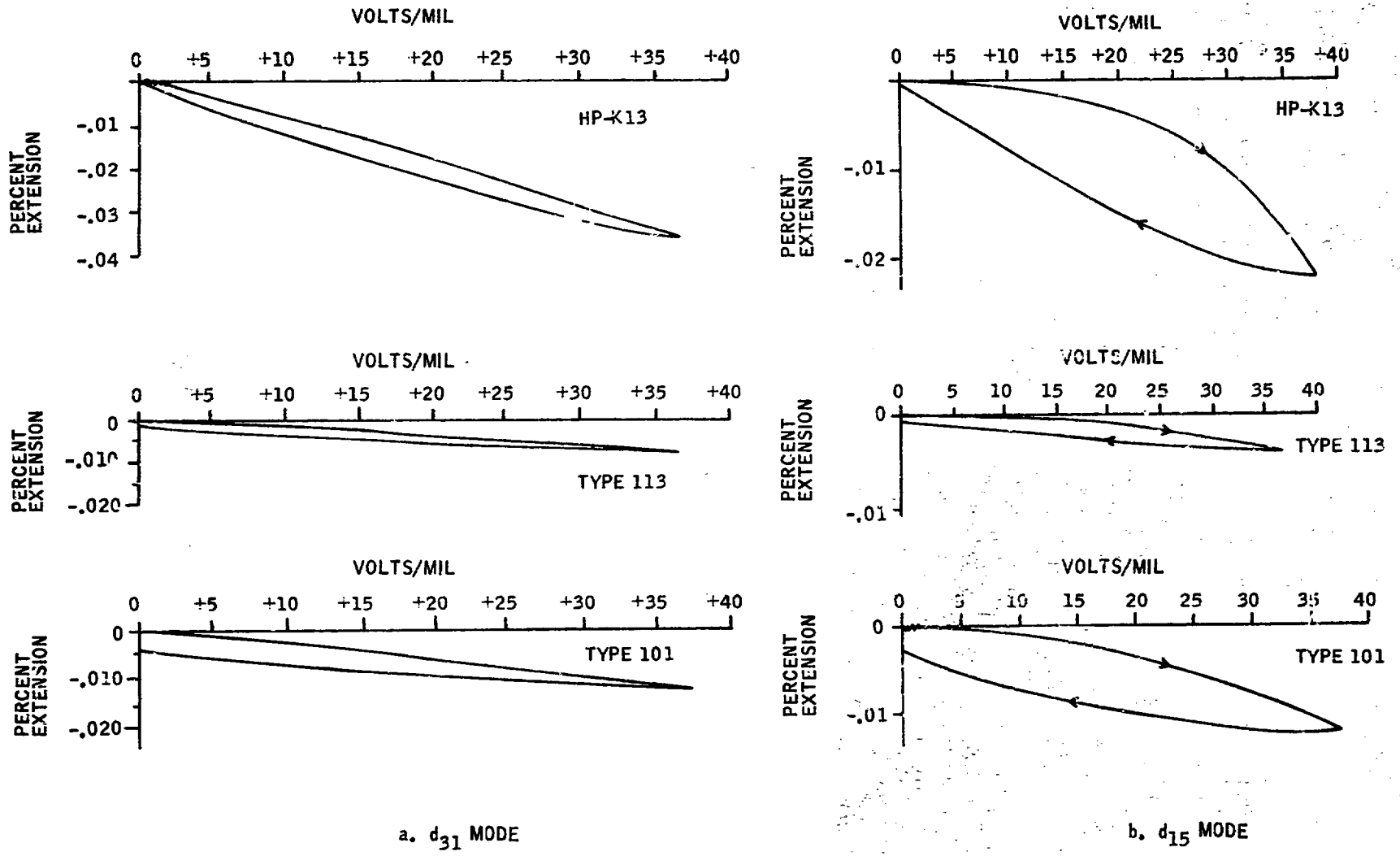

a. d_{31} MODE

b. d_{15} MODE

Figure 10. Field versus extension (half loop) for poled material.

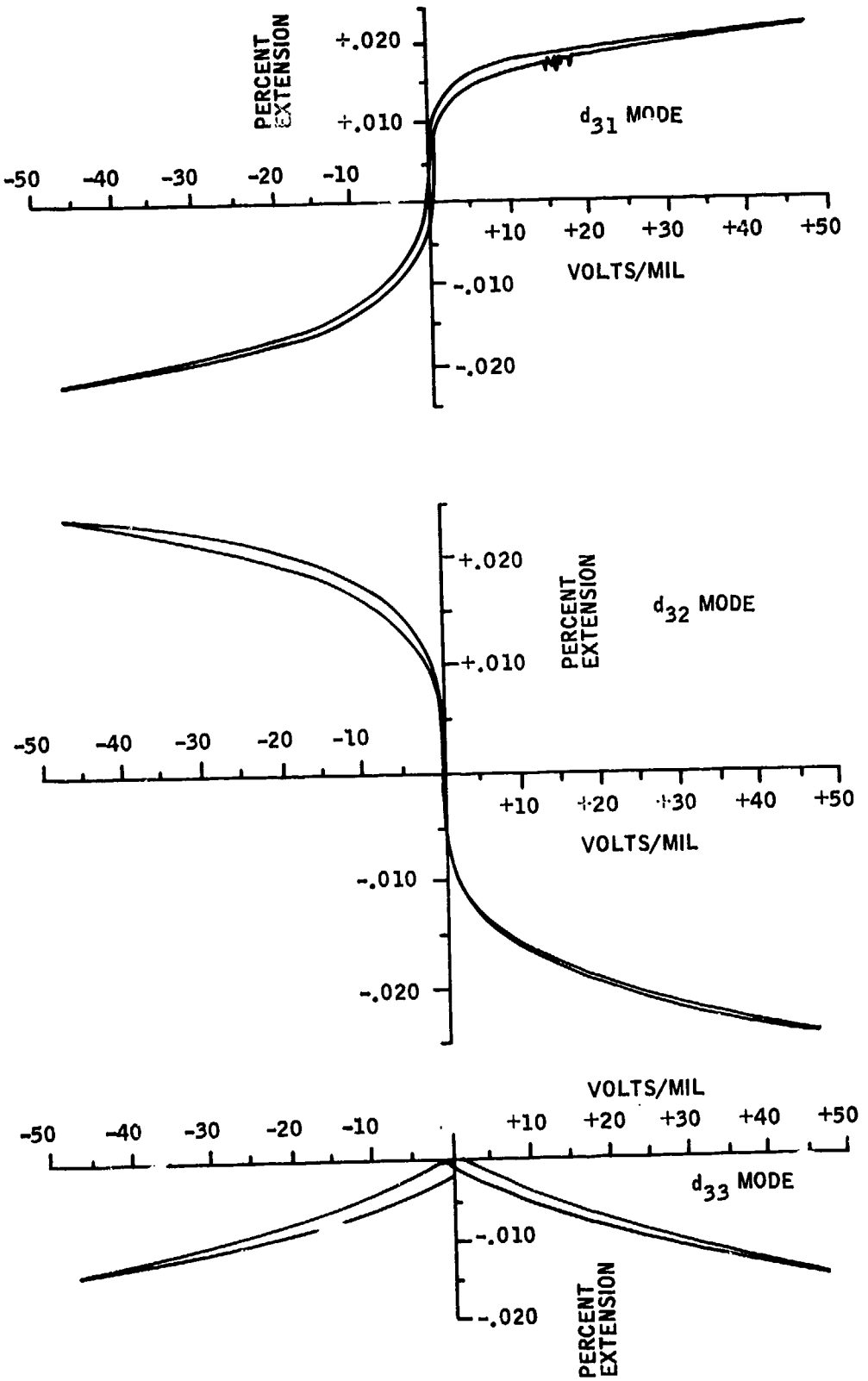

Figure 11. Field versus extension of single crystal Rochelle salt.

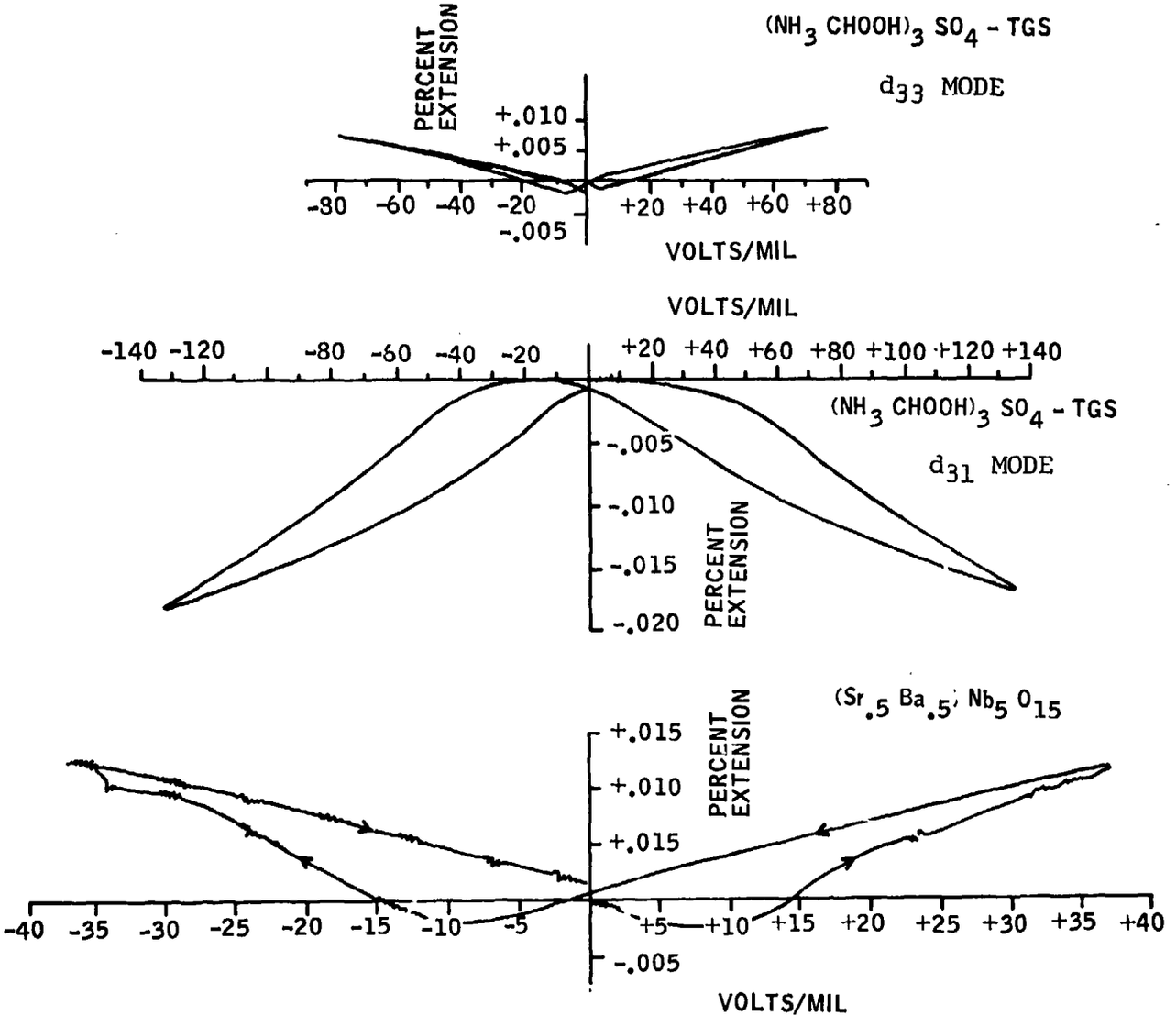

Figure 12. Field versus extension character of $(Sr_{.5} Ba_{.5}) Nb_5O_{15}$ and $(NH_3CHOOH)_3 SO_4$.

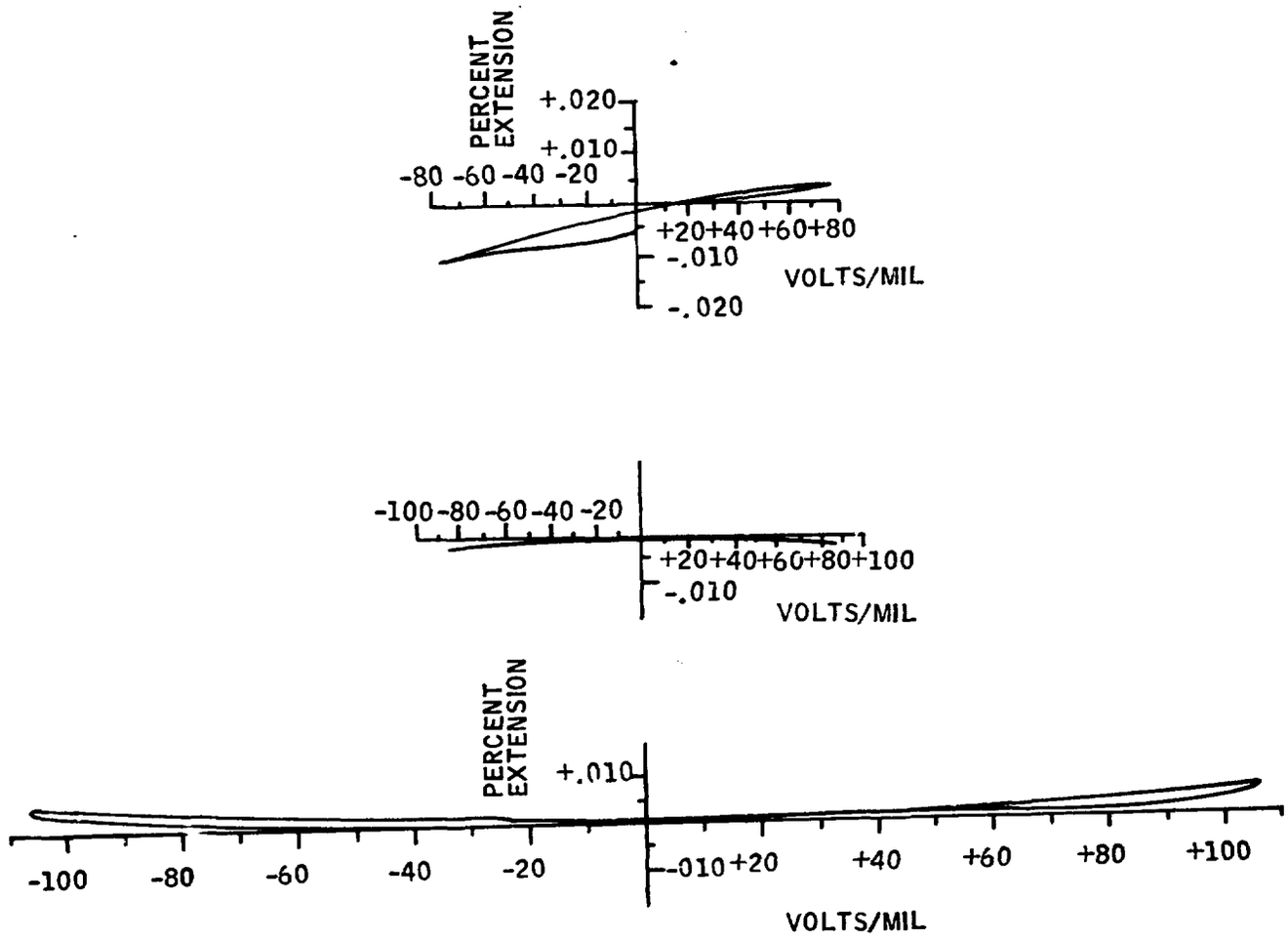

Figure 13. Field versus extension character of $KTaO_3$, $LiNbO_3$ and $LiGaO_2$ d_{33} mode.

strain was produced in the d_{31} direction. Figure 12 also shows data for a $(Sr_{0.5}Ba_{0.5})Nb_5O_{15}$ (SBN) single crystal which had fairly high d_{33} expansion; and the average atomic mass was slightly less than PZ-PT, but large crystals are very difficult and costly to produce. Figure 13 shows the low displacements obtained for the other three materials.

The materials which appear to offer the most promise are the $(K_{0.5}Na_{0.5})NbO_3$ and $(Na_{0.8}Cd_{0.1})NbO_3$ type ceramic materials with a Z of 34. The d_{33} of these materials may exceed 200, their Curie temperature is much higher than $BaTiO_3$ (Z of 47) and their molecular structure contains no hydroxyl ions. Additional efforts are necessary to attempt to make ceramic formulations of these NbO_3 base piezoelectric ceramic materials.

Radiation Resistance

The radiation resistance of many of these materials has been studied previously, however, we were unable to find any work that studied more than one type of ferroelectric type material at a time.

Ruffing[17] summarizes the effort in electrical materials. In general, metals where electron mobility is quite high take very large amounts of radiation energy to produce any significant structural changes other than heating. In organic materials, physical or chemical deterioration usually takes place before appreciable changes in electrical properties occur. Radiation resistance does depend strongly on the temperature capability of the material because induced heating can destroy cross-linked and chain-scission type organics such as a PVF_2 polymer. Doses up to 10^5 rads usually show little or no effect after radiation but electrical resistance in polymers can decrease 100-1000 times during radiation. Ruffing indicates that epoxies are only good to about 10^6 rads without fillers but improve (10^7 - 10^8 rads) with fillers. Also, mica is reported to be damaged by x-rays (210 KV and 20 ma) where destruction of secondary bonding at crystal faces was caused by the loss of free OH groups. The formation of f-centers and free electrons were put into the crystal lattice at defects.

As discussed earlier, it appears that peculiar changes in the polarization behavior of these materials occur when they are exposed to ionizing radiation (x-rays and

electrons). Most of these changes do not appear to be permanent except possibly where weak, chemically bound hydroxyl materials are present in the crystal structure such as in Rochelle salt.

In all of the articles reviewed[25-33] concerning the radiation resistance of PZ-PT[28,29] and other piezoelectric type materials, the authors have shown significant changes occur in remnant and saturation polarization and coercive field (this was referred to as switching field earlier). In single crystal materials such as $BaTiO_3$,[27] TGS,[26] Rochelle Salt,[25] and $(NaK)NbO_3$[33] polarization versus field loops were deformed and double hysteresis loops appeared for fast neutron dosages above 10^{12} nvt. This effect was also seen in TGS subjected to ionizing radiations (x-rays and electrons) from an x-ray tube running at only 30 KV and 20 ma and to a detectable degree even at an 8 KV and 15 ma level after several hours. Chynoweth[26] suggests that the effects are caused by the gradual increase of strain in the crystal.

In general, as exposure times are increased, the coercive field (E_c) decreases and eventually polarization decreases. Since the amount of polarization present is directly related to the piezoelectric strain constant, the displacement in a PLC type transducer will be decreased.

The effects noted are somewhat typical of simple heating of these crystals. For instance, when PZ-PT is heated, E_c decreases and polarization decreases as the Curie temperature is approached. In certain mixed phase PZ-PT structures, a double hysteresis loop may also be obtained. Thus, simple heating by ionization radiations is expected to be the primary cause of PLC instability in the laser gyro. The properties which need to be modified are:

- Reduction of the average atomic mass which will decrease the amount of radiation induced heating.
- Increasing the temperature stability of the piezoelectric properties to improve the micropositioning stability of the transducer. This can be obtained by:
  - Increasing the Curie temperature
  - Increasing the coercive field
  - Stabilizing d_{33} and d_{31} outputs with temperature.

RECOMMENDATIONS

The best material presently available for this purpose is probably type 113 $BaTiO_3$ or a temperature stable PZ-PT such as used in piezoelectric band-pass filters. Both of these will produce less displacement for a given drive voltage than the presently used hot pressed K-13 PZ-PT; however, design changes in the transducer as discussed below are expected to compensate for these reductions. New materials such as $(Na_{0.5}K_{0.5})NbO_3$ and $(Na_{0.8}Cd_{0.1})NbO_3$ or combinations of these also should be more thoroughly evaluated for their field versus train temperature stability. This is also particularly important because it would improve the functional stability of the gyro over other non-radiation sensitivity improvements.

PLC TRANSDUCER DESIGN

Seven potential design configurations for the path length control (PLC) transducer have been initially examined which could utilize the new low Z materials analyzed under this program. Seven representative design configurations are shown in Figure 4 and Figures 14 through 18. These take several different approaches to the problem and can be combined as desired to achieve maximum benefits.

In all these designs, a standard method of electroding is shown. The piezoelectric ceramic shapes contain fired silver electrodes. External electrical contacts are achieved by cementing a thin metallic electrode to the silver which can be soldered to copper lead wires.

Since the existing design is the one which is known the best, it will be used as the control as well as a potential candidate for future application. The only change is to reduce the diaphram thickness to permit greater throw with piezoelectric materials with lower d_{31} or less throw efficiency. This configuration is shown in Figure 4. A variation in this design is shown in Figure 13 where the driver assembly is bonded to the transducer (mirror) instead of using a mechanical linkage. This should produce greater throw efficiency; however, previously used bonded structures of this type have experienced bond failures.

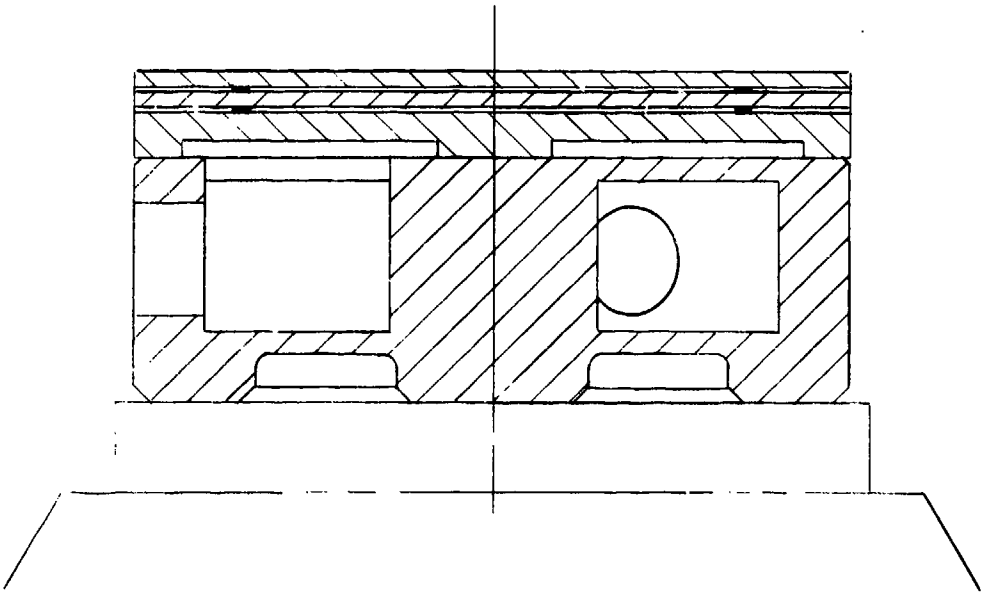

Figure 14. PLC transducer - cemented configuration.

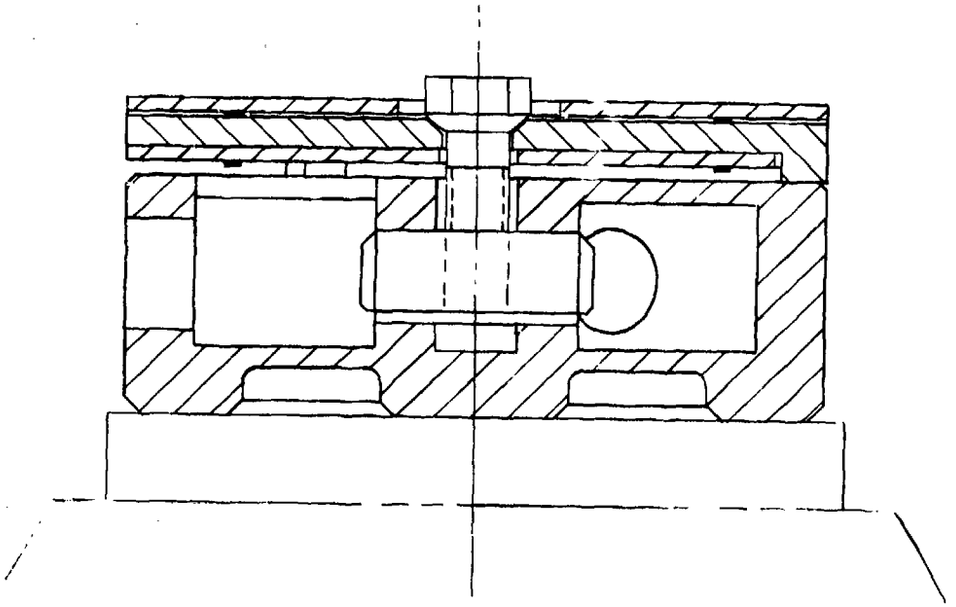

Figure 15. PLC transducer - top and bottom driver.

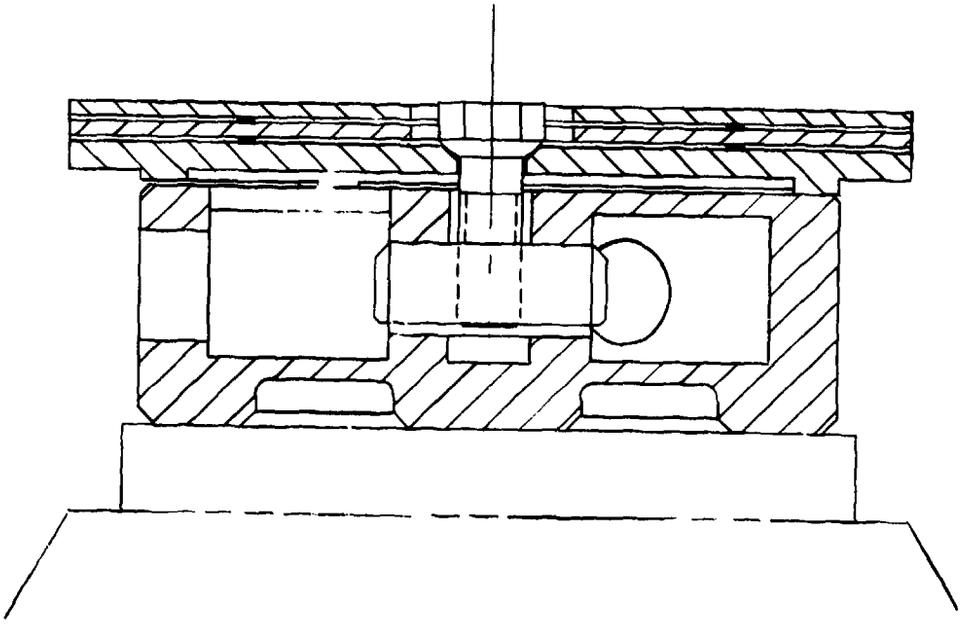

Figure 16. PLC transducer - large diameter driver.

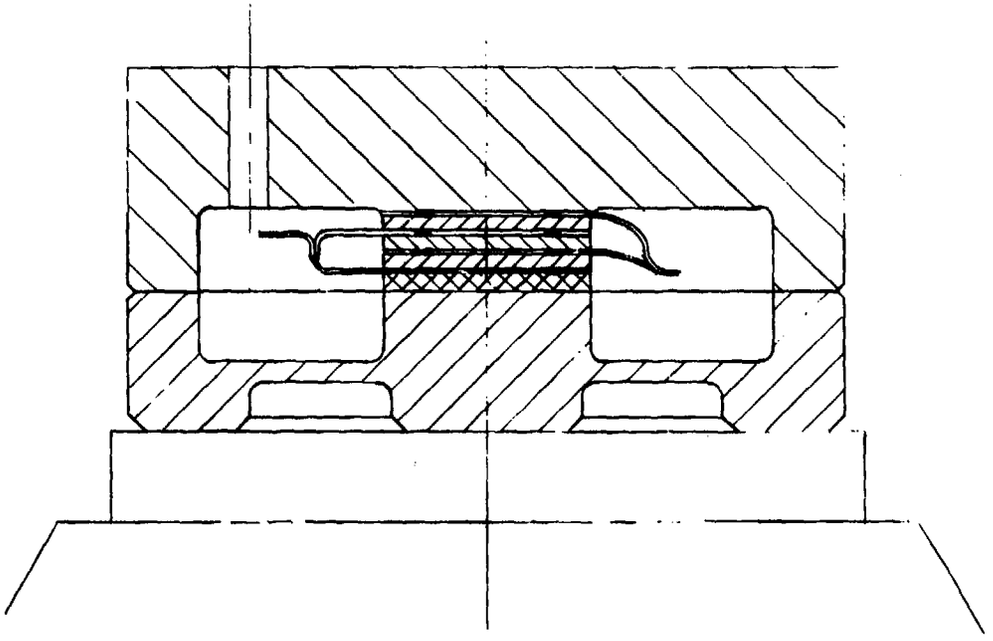

Figure 17. PLC transducer - d_{33} center stack.

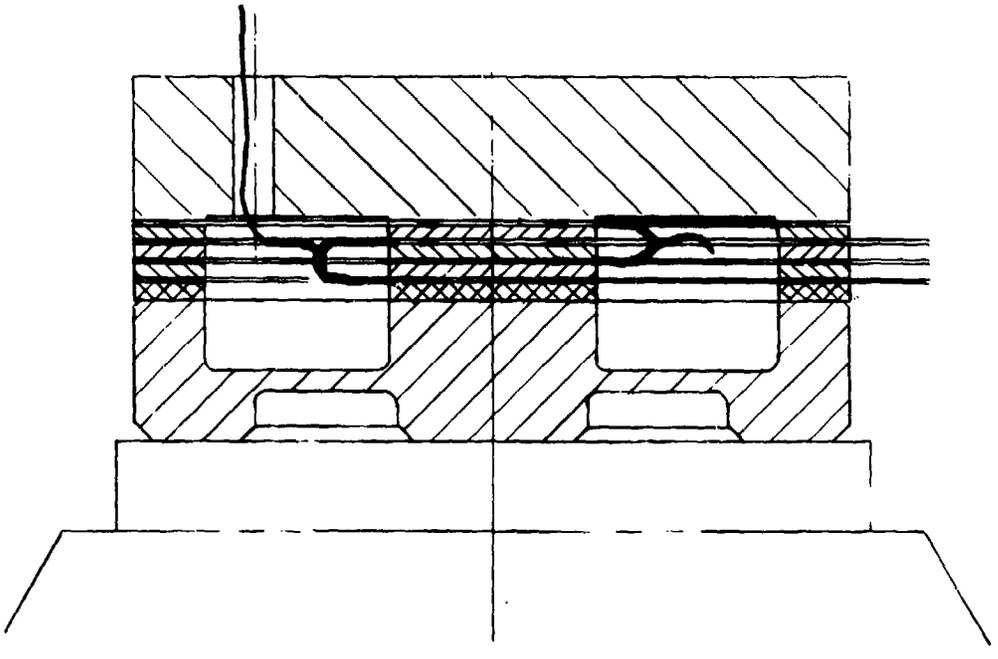

Figure 18. PLC transducer - d_{33} center and washer stacks.

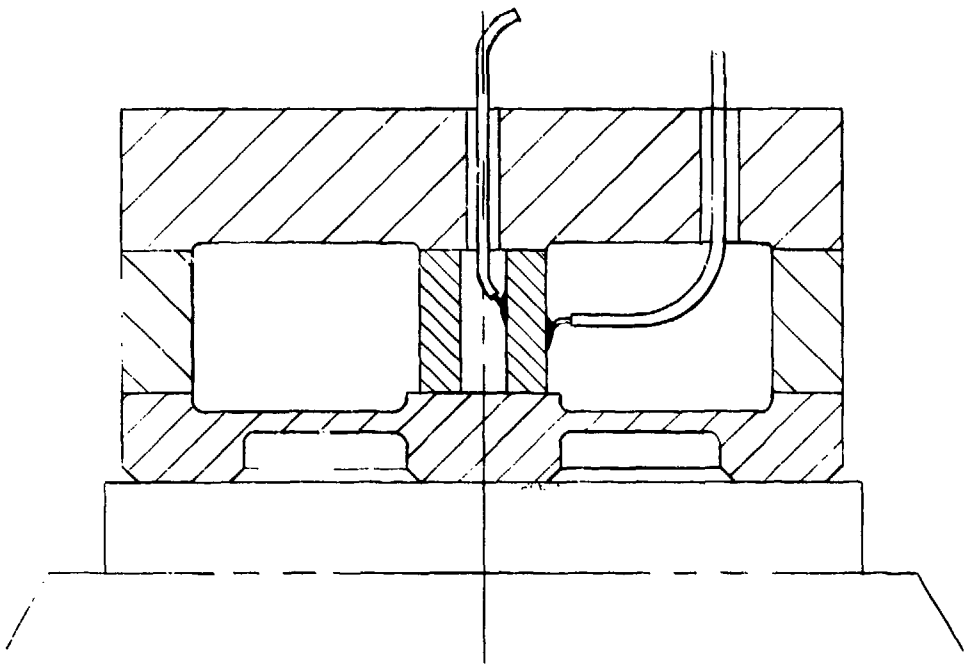

Figure 19. PLC transducer - d_{31} center cylinder.

Since the apparent result of the radiation in causing a failure mode is to absorb radiation, the present effort has concentrated on finding less absorptive material. However, since the heating deformation action is the real failure causing mode, design changes can be made to mitigate this result. Top and bottom mounted piezoelectric elements would both tend to heat as a result of radiation and their temperature increase would tend to compensate or cancel the motion-producing effect. An approach which uses this technique is shown in Figure 15. A variation of this technique would be to use a single crystal as the driver to reduce the bimetallic effect from the present two layer sandwich.

Another approach would be to utilize two separate PLC transducers each thermally compensated to move in opposite directions to provide total path length-compensation. This design may be more difficult to control and evaluate, for which reason it will not be considered in this study.

Since the most significant anticipated result of using a low Z piezoelectric material is lower throw efficiency, another technique would be to increase the area of the crystal(s) to obtain greater throw. Approximately 50 percent increase in crystal area can be achieved without the device becoming excessively large. There is the trade off, however, which must be made of increased area (i.e., material), and sensitivity to irradiation even though the Z number is reduced. A representation of this approach is shown in Figure 16.

Another class of driver is shown in Figure 17. It utilizes the expansion/contraction of a piezo stack for direct actuation of the mirror. The internal version would benefit from additional shielding inside and/or outside the transducer. Also, its small volume would minimize radiation absorption. An approach which is more complicated, but holds promise of both greater throw and self compensation from heating is shown in Figure 18. Here the crystal heating resulting from irradiation will tend to cancel the resulting motion of the element stacks. The normal operation of push/pull should also amplify motion from available voltages to maximize throw.

The effect of shear poling was demonstrated during the first phase of this program and gives rise to the device shown in Figure 16. The slug has been refined to a hollow cylinder. It is shown in a similar design to the inside element stack of Figure 17. Its simplicity is attractive. The use of inside/outside cylinders for thermal compensation and maximized throw would probably be the better configuration of this type of driver.

The versions proposed for study in any future effort include 1) the top and bottom element standard design, 2) the internal/external stack and 3) the internal/external d_{15} or d_{31} poled cylinder approach.

These self-compensating versions appear to hold the most promise of thermal insensitivity both to normal and radiation environments.

SECTION 3
CONCLUSIONS

Three lower average atomic mass piezoelectric ceramic materials were identified in this program which appear to have sufficient field-versus-displacement to be used in place of the present lead zirconate-lead titanate in the driver section of the path length control (PLC) transducer. Sodium potassium niobate and sodium cadmium niobate have about one half the average atomic mass of the presently used material while the more common barium titanate materials are two-thirds less. Both materials have lower displacement coefficients (d_{31}) but more efficient transducers have been designed which appear to compensate for this lower motion. While many other materials were identified which had significantly lower average atomic masses, their displacement coefficients were too low to be of use in the transducer. One material, TGS containing hydroxyl ions, may also deserve further study because the radiation sensitivity of this material is not well known.

SECTION 4
RECOMMENDATIONS

It is recommended that two types of $BaTiO_3$ be used to study the performance of these two materials in at least three new PLC transducers. Prototype models of these designs should be built and evaluated to determine their path length control capability. Simultaneous to this effort, a standard hot pressing process should be used to produce the sodium potassium (and cadmium) niobate piezoelectric ceramic elements. The actual displacement characteristics of these should be optimized and this material should then be evaluated and compared to single crystal TGS in the most appropriate design found with the $BaTiO_3$. The function of a laser gyro with these prototype PLC transducers should then be evaluated under ambient and a high radiation environment.

REFERENCES

1. Jaffe, B., W.R. Cook and H. Jaffe: "Piezoelectric Ceramics," Academic Press (1971).

2. Cleveland Crystals, Inc. Company literature and personal communication with William R. Cook, Jr.

3. American Institute of Physics Handbook, 2nd Edition, McGraw-Hill (1963).

4. Pulvari. "Ferroelectric Materials Survey with Particular Interest in their Use at High Temperatures," WADS Tech. Note 56-467, Feb. 1957.

5. Tamura, et. al. "Piezoelectricity in Uniaxially Stretched Poly (vinylidene fluoride) Films and Its Application," Ferroelectrics, 10 P125 (1976).

6. Skinner, et al. "Flexible Composite Transducers," Materials Research Laboratory, The Pennsylvania State University.

7. Austerman, et al. "Polar Properties of BeO Single Crystals." JAP, 34 (2) p. 339 (1963).

8. O.E. Mattiat, ed. "Ultrasonic Transducer Materials," Plenum Press (1971).

9. W.G. Cady. "Piezoelectricity" Vol. 1-2. Dover Publications (1964).

10. Adhav. Elastic, Piezoelectric and Dielectric Properties of Rubidium Dihydrogen Phosphate. JAP, 40 (7) p. 2725 (1969).

11. Uematsu and Koide. "Piezoelectric Properties of Ferroelectric $K_3Li_2(Ta_xNb_{1-x})_5O_{15}$ Single Crystals." Jap. J. Appl. Phys., 9 (3) p. 336 (1970).

12. CRC Handbook of Materials Science; Vol. III, Nonmetallic Materials and Applications. Charles T. Lynch, CRC Press (1975).

13. Jaeger and Egerton. "Hot Pressing of Potassium Sodium Niobates," J. Am. Cer. Soc., 45 p. 209 (1962).

14. Warner, et al. "Piezoelectric and Photoelastic Properties of Lithium Iodate." J. Acoust. Soc. Am., 47 p. 791 (1970).

15. Fukomoto and Watanabe. "Elastic and Piezoelectric Constants of $Sr_4KLiNb_{10}O_{30}$ Type Ferroelectric Crystal." Proc. IEEE, 58 (9) p. 1376 (1970).

16. Liu. "Technical Report of Dielectrics and Intermetallics," Honeywell Corporate Materials Science Center, Apr. 1978.

17. Warner, et al. "Elastic and Piezoelectric Constants of Ba_2NaNb_5-O_{15}." JAP, 40 (11) p. 4353 (1969).

18. Liu and Maciolek, Patent Specification 1466387.

19. Honeywell Ceramics Center Bulletin

20. Yamada, et al. "Piezoelectric and Elastic Properties of LiTaO3-- Temperature Characteristics." JAP. J. Appl. Phys. 8 (9) p. 1127 (1969).

21. Yamada and Iwasaki. "Ferroelectric, Piezoelectric, and Optical Properties of $SrTeO_3$ Single Crystals and Phase-Transition Points in the Solid Solution Systems." JAP, 44 (9) p. 3934 (1973).

22. Chubachi, et al. "Influence of Dislocations in CdS Crystal on its Electro-mechanical Coupling Factors." JAP, 42 (3) p. 962 (1971).

23. Charlson and Mott: "Piezoelectricity Constants of Gallium Arsenide." Proc. IEEE, 51 (9) p. 1239 (1963).

24. Private Communication from B. Passenheim, Mission Research Corporation, La Jolla, California.

25. Urin. Izvest. Akad. Nauk, SSSR. Ser. Fiz, 21, p. 329 (1957)

26. Chynoweth. "Radiation Damage Effects in Ferroelectric Triglycise Sulfate," Phys. Rev. 113 (1) 159-66 (1959).

27. Lefkowitz and Mitsui. "Effect of X-ray and Pile Irradiation on the Coercive Field of $BaTiO_3$," J. Appl. Phys 30 (1) 269 (1959).

28. Glower, Hester and Warnke "Effects of Radiation-Induced Damage Centers in Lead Zirconate Titanate Ceramics," J. Am. Ceram. Soc. 48 (8) 417-21 (1965)

29. Glower and Hester "Effects of Radiation-Induxed Damage Centers in Lead Zirconate Titanate Ceramics." J. Appl. Phys. 36, 2175 (1965).

30. Hilczar. Phys. Status Solidi 5, 113 (1964).

31. Schenk. Phys. Status Solidi 4, 25 (1964).

32. Ruffing. "Radiation Effects on Electrical/Electronic Materials," Insulation/Circuits, p 23 (1971).

33. Cross. Phil. Mag. 1, p 76 (1956).

34. Noble, Callaghan, Passenheim "Dins Phase I Surviability and Vulnerability," Final Report to DNA, October 1977.

SELECTED BIBLIOGRAPHY

Adhav. "Piezoelectric Effect in Tetragonal Crystals." JAP, 46, No. 6, 1975, p. 2808.

Aizu. "Possible Species of Ferroelectrics." Phys. Rev., 146, No. 2, 1966, p. 423.

Albers, et al. "Dielectric, Elastic and Piezoelectric Properties of Mg-Cl Boracite." Phys. Status Solidi A, 36, No. 1, 1976, p, 189.

Avakian, et al. "Spontaneous Electric Breakdown in Pyroelectric $LiNbO_3$ and $LiTaO_3$ Crystals," Phys. Status Solidi A, 36, No. 1, 1976, p. K2S.

Battle and Marino. Development of Manufacturing Process for High-Purity Electronic Ceramics. AD 270203 and AD 276868.

Bauer, et al. "Ferroelectric Ceramics - Application to Mechanical-Electrical Energy Conversion Under Shock Compression." Ferroelectrics, 10, Nos. 1-4, 1976, p. 61.

Bergman, et al. "Curie Temperature, Birefringence, and Phase Matching Temperature in $LiNbO_3$ as a Function of Melt Stoichiometry." Appl. Phys. Letters, 12, No. 3, 1968, p. 92.

Berlincourt. "Current Developments in Piezoelectric Applications of Ferroelectrics." Ferroelectrics, 10, Nos. 1-4, 1976, p. 111

Bernard, et al. "New Ferroelectric Composition $Cd_2Nb_2O_6S$." (Fr.) Mat. Res. Bull., 6, No. 2, 1971, p. 75.

Bernstein, "Piezoelectric Langbeinite-Type $K_2Cd_2(SO_4)_3$ - - -." Jour. of Chem. Phys., 67, No. 5, 1977, p. 2146.

Burns, et al. "Ferroelectric Properties of the $KSr_2Nb_5O_{15}$-$LaNb_3O_9$ System." Solid State Commun., 6, No. 4, 1968, p. 223.

Bertaut, et al. "Rate Earth and Yttrium Manganates--A New Class of Ferroelectrics." Comp. Rend., 256, No. 9, 1963, p. 1958.

Chan Van Thieu, et al. "Structure and Dielectric Properties of Some Li-Containing Perovskites." Izv. Acad. Nauk SSSR Neorg. Mater., 8, No. 9, 1972, p. 1631.

Chi and Sladek. "Elastic Constants and the Electrical Transition in Ti_2O_3." Phys. Rev. B, 7, No. 12, 1973, p. 5080.

Chung, et al. "Redetermination of Elastic Constants of Single-Crystal $CaMoO_4$." JAP, 44, No. 5, 1973, p. 2424.

Clark. "Rare Earth Pressure Transducers." Instru. Control Systems, 36, No. 2, 1963, p. 93.

Connally and Turner. "Ferroelectric Materials and Ferroelectricity." of Solid State Physics Literature Guides, Vol. 1, Plenum Press, 1979.

Dangier, et al. "Magnetic, Electrical and Optical Properties of the Perovskite-Type Phases $SrVO_{2.9}$ and $SrVC_3$." Jour. Solid State Chem., 14, No. 3, 1975, p. 247.

Foster. "Application of Piezoelectric Semiconductors to the Fabrication of High Frequency Ultrasonic Transducers." Trans. AIME 230, No. 7, 1964, p. 1503.

Galasso, F.S. Structure, Properties and Preparation of Perovskite-Type Compounds, Pergamon Press, 1969.

Ganekar and Sladek. "Piezoresistance and Piezo-Hall Effects in n- and p-Type Aluminum Antimonide." Phys. Rev., 146, No. 2, 1966, p. 505.

Haerdtl. "Physics of Ferroelectric Ceramics Used in Electronic Devices." Ferroelectrics, 12, Nos. 1-4, 1976, p.9.

Haertling. "Properties of Hot-Pressed Ferroelectric Alkalide Niobate Ceramics." Jour. Am. Cer. Soc., 50, No. 6, 1967, p. 329.

Hoc.,ins and Irwin. "Elastic Constants of ZnSe." Phys. Status Solidi A, 28, No. 2, 1975, p. 647.

Iwasaki, et al. "Piezoelectric and Optical Properties of $LiNbO_3$ Single Crystals," Rev. Elec. Commun. Lab. (Tokyo), 16, Nos. 5-6, 1968, p. 385.

Jhunijhunwala, et al. "Berlinite, A Temperature Compensated Material for Surface Acoustic Wave Applications." Jour. Applied Phys., 48, No. 3, 1977, p. 887.

Kasimov. "Magnetic and Electrical Properties of Partly Reduced Nb_2O_5." Azv. Acad. Nauk SSSR Neorg. Mater., 12, No. 3, 1976, p. 546.

Kell. "Properties of Niobate High Temperature Piezoelectric Ceramics." Proc. Inst. Elec. Engrs. (London) Pt. B, 109, No. 22, London, 1962, p. 369.

Khromova. "Elastic, Piezoelectric, and Dielectric Constants of Multi-Domain and Nonstoichiometric $LiNbO_3$ Crystals." Izv Akad. Nauk SSSR Neorg. Mater., 11, No. 8, 1975, p. 1444.

Kimura, et al. "Ferroelastic Behavior in $Ba_2Ge_2TiO_8$." JAP, 47, No. 6, 1976, p. 2249.

Lane and Brown. "Piezoelectric, Pyroelectric, and Dielectric Properties of Thin Ceramic Elements." Trans. Jour. Brit. Ceram. Soc., 73, No. 3, 1974, p. 65.

Lindquist. "Latest Fundamentals of Piezoelectric Ceramics." Ceram. Ind., 80, No. 5, 1963, p. 56.

Luff, et al. "Ferroelectric Ceramics with High Pyroelectric Properties." Trans. Jour. Brit. Ceram. Soc., 73, No. 7, 1974, p. 251.

Martin. "Piezoelectricity." Phys. Rev. B., 5, No. 4, 1972, p. 1607.

Mason, W.P. Electromechanical Transducers and Wave Filters. D. Van Nostrand Company, Inc., 1948.

Matsuura and Tsurumi. "Effects of Uniazial Stress on the Electrical Properties in CdS Single Crystals." Jour Phys. Soc. Jpn., 39, No. 6, 1975, p. 1543.

Nassau, et al. "Domain Structure and Etching of Ferroelectric Lithium Borate." Appl. Phys. Letters, 6, No. 11, 1965, p. 228.

Nitta. "Properties of Sodium-Lithium Niobate Solid Solution Ceramics with Small Li Concentrations." Jour. Am. Ceram. Soc., 51, No. 11, 1968, p. 626.

Notis, et al. "Elastic, Magnetic and Electrical Properties of Pure and Li-Doped Nickel Oxide." JAP, 44, No. 9, 1973, p. 4165.

"Numerical Data and Functional Relationships in Science and Technology." Landolt-Boernstein (New Series). K. H. Hellewege, Ed. -in Chief. Group III, Crystal and Solid State Physics; Vol. 2, Elastic, Piezoelectric, Piezooptic, Electro-optic Constants, and Non-linear Dielectric Susceptibilities of Crystals. R. Bechmann, et al, Springer-Verlag, 1969.

Okazaki and Nagata. "Relation Between Grain Density and Size, and the Piezoelectric Properties of Ceramics Based on Pb, Zr, and Ti." Ceram. Ind. (Faenza), 12, No. 4, 1977, p. 173.

Opriou, et al. "Effect of Radiation on the Electrical Properties of Some Dielectric Materials." Stud. Cercet. Fiz., 24, No. 9, 1972, p. 1179.

Pepinsky and Vedam. "$LiH_3(SeO_3)_2$ -- A New Room-Temperature Ferroelectric." Phys. Rev., 114, No. 5, 1959, p. 1217.

Pulvari. "Research on High Temperature Ferroelectric Storage Media." WADD Tech. Report, Apr. 1960, p. 60-146.

"Radiation Damage in Solids." Part of the Proceedings of the Symposium on Radiation Damage in Solids and Reactor Materials Held by the International Atomic Energy Agency, Venice, May 1962: I-III, 1962-1963. (See especially Vol. II).

Roy. "Mechanical Responses in a Piezoelectric Plate Transducer." Indian Jour. Pure Appl. Phys., 5 No. 4, 1967, p. 152.

Sager and Rubenstein. "Piezoresistance in n-Type CdTe." Phys. Rev., 143, No. 2, 1966, p. 552.

Sasaki, et al. "Photoelastic Effect in Piezoelectric Semiconductor ZnO." JAP, 47, No. 5, 1976, p. 2046.

Schmidt, et al. "Piezoelectricity of $NaH_3(SeO_3)_2$ Crystals." Phys. Status Solidi A, 29, No. 1, 1975, p. K65.

Sharma and McCartney. "Dielectric Properties of Pure $BaTiO_3$ as a Function of Grain Size." Jour. Aust. Ceram. Soc., 10, No. 1, 1974, p. 16.

Smolenskii, et al. "New Ferroelectrics of Complex Compositions: IV. Sov. Phys. -Solid State, 2, No. 11, 1960, p. 2651.

Sonin and Zheludev. "Search for New Ferroelectrics and Antiferroelectrics not Belonging to the Oxide Group."

Sorge, et al. "Dielectric, Elastic and Piezoelectric Properties of $NaH_3(SeO_3)_2$ Crystals Near the α/β Transition." Phys. Status Solidi A, 21, No. 2, 1974, p. 463.

Thomann and Heydrich. "$BaTiO_3$ Ceramics Without Hysteriesis." Ferroelectrics, 7, Nos. 1-4, 1974, p. 357.

Tufte and Stelzer. "Piezoresistance Properties of Reduced Strontium Titanate." Phys. Rev., 141, No. 2, 1966, p. 675.

Uchida and Ikeda. "Electrostriction in Perovskite-Type Ferroelectric Ceramics." JAP, Jour. Appl. Phys., 6, No. 9, 1967, p. 1079.

Uchida and Saito. "Elastic and Photoelastic Constants of α-ZnS." JAP, 43, No. 3, 1972, p. 971.

Uesu and Kobayashi. "Crystal Structure and Ferroelectricity of CsH_2P_4." Physics Status Solidi A, 34, No. 2, 1976, p. 475.

Vedam and Davis. "Piezo- and Thermo-Optic Behavior of $LiNbO_3$." Appl. Phys. Letters, 12,, No. 4, 1968, p. 138.

Verbitskaya. "Investigation of Electrostriction of Seignette Ceramics." Dok, Acad. Nauk SSSR, 114, No. 3, 1957, p. 533, (Russ.).

Weider, et al. "Ferroelectric and Pyroelectric Properties of Mineral and Synthetic Colemanite ($2CaO \cdot 3B_2O_3 \cdot 5H_2O$)." JAP, 33, No. 5, 1962, p. 1720.

Weirauch and Tennery. "Electrical, X-ray and Thermal Expansion Studies in the System $KNbO_3$-$AgNbO_3$." Jour. Am. Ceram. Soc., 50, No. 11, 1968, p. 626.

DISTRIBUTION LIST

DEPARTMENT OF DEFENSE

Assistant to the Secretary of Defense
Atomic Energy
ATTN: Executive Assistant

Command and Control Technical Center
ATTN: C-362, G. Adkins

Defense Technical Information Center
12 cy ATTN: DD

Defense Electronic Supply Center
ATTN: DESC-ECT, J. Niles
ATTN: DESC-ECS, D. Hill
ATTN: DESC-ECS, J. Dennis
ATTN: DESC-EQM, R. Grillmeier
ATTN: DESC-ECP, D. More
ATTN: DESC-ECT, D. Droege
ATTN: DESC-ECS, J. Counsil

Assistant Secretary of Defense
Program Analysis & Evaluation
ATTN: M. Doffredo

Defense Logistics Agency
ATTN: DLA-SE
ATTN: DLA-QEL, J. Slattery

Defense Material Specifications & Standard Office
ATTN: L. Fox

Defense Nuclear Agency
ATTN: RAEV, M. Kemp
ATTN: DDST
ATTN: RAAE, H. Fitz, Jr.
4 cy ATTN: TITL

Field Command
Defense Nuclear Agency
ATTN: FCPR

Field Command
Defense Nuclear Agency
Livermore Division
ATTN: FCPRL

National Security Agency
ATTN: T. Brown
ATTN: P. Deboy
ATTN: G. Daily

NATO School (SHAPE)
ATTN: U.S. Documents Officer

Undersecretary of Defense for Rsch., & Engrg.
ATTN: Strategic & Space Systems (OS)

DEPARTMENT OF THE ARMY

Aberdeen Proving Ground
Department of the Army
ATTN: S. Harrison

Bmd Advanced Technology Center
Department of the Army
ATTN: ATC-T

DEPARTMENT OF THE ARMY (Continued)

BMD Systems Command
Department of the Army
ATTN: BMDSC-HW, R. DeKalb

Deputy Chief of Staff for Research, Dev., & Acq.
Department of the Army
ATTN: Advisor for RDA Analysis, M. Gale

Harry Diamond Laboratories
Department of the Army
ATTN: DELHD-N-RBH
ATTN: DELHD-N-RBC, J. McGarrity
ATTN: DELHD-N-RBH, J. Halpin
ATTN: DELHD-N-RBH, H. Eisen
ATTN: DELHD-N-P, F. Balicki
ATTN: DELHD-N-P

U.S. Army Armament Research & Development Command
ATTN: DRDAR-LCA-PD

U.S. Army Communications R&D Command
ATTN: D. Huewe

U.S. Army Missile R&D Command
3 cy ATTN: RSIC

U.S. Army Nuclear & Chemical Agency
ATTN: Library

White Sands Missile Range
Department of the Army
ATTN: STEWS-TE-AN, T. Leura
ATTN: STEWS-TE-AN, M. Squires

DEPARTMENT OF THE NAVY

Naval Air Systems Command
ATTN: AIR 350F

Naval Electronic Systems Command
ATTN: Code 5045.11, C. Suman

Naval Ocean Systems Center
ATTN: Code 4471

Naval Postgraduate School
ATTN: Code 0142
ATTN: Code 1424

Naval Research Laboratory
ATTN: Code 5216, H. Hughes
ATTN: Code 6627, C. Guenzer
ATTN: Code 6650, A. Navenson
ATTN: Code 5210, J. Davey
ATTN: Code 6701, J. Brown
ATTN: Code 6601, E. Wolicki
ATTN: Code 6600, J. McElliney

Naval Sea Systems Command
ATTN: SEA-06J, R. Lane

Naval Ship Engineering Center
ATTN: Code 6174D2

DEPARTMENT OF THE NAVY (Continued)

Naval Surface Weapons Center
ATTN: Code F30
ATTN: Code F31

Naval Weapons Center
ATTN: Code 233

Naval Weapons Evaluation Facility
ATTN: Code AT-6

Naval Weapons Support Center
ATTN: Code 7024, J. Ramsey
ATTN: Code 7024, T. Ellis
ATTN: Code 70242, J. Munarin

Office of Naval Research
ATTN: Code 427, L. Cooper
ATTN: Code 220, D. Lewis

Office of the Chief of Naval Operations
ATTN: OP 985F

Strategic Systems Project Office
Department of the Navy
ATTN: NSP-27331, P. Spector
ATTN: NSP-2701, J. Pitsenberger
ATTN: NSP-2015
ATTN: NSP-230, D. Gold

DEPARTMENT OF THE AIR FORCE

Air Force Aero-Propulsion Laboratory
ATTN: POD, P. Stover

Air Force Avionics Laboratory
ATTN: TEA, R. Conklin
ATTN: DHE, H. Hennecke

Air Force Geophysics Laboratory
ATTN: SULL
ATTN: SULL S-29

Air Force Institute of Technology
Air University
ATTN: ENP, C. Bridgeman

Air Force Materials Laboratory
ATTN: LTE
ATTN: LPO, R. Hickmott

Air Force Systems Command
ATTN: DLCAM, T. Seale
ATTN: DLCA
ATTN: DLW
ATTN: XRLA, R. Stead

Air Force Technical Applications Center
ATTN: TAE

Air Force Weapons Laboratory
Air Force Systems Command
ATTN: ELP, M. Knoll
ATTN: ELT, J. Ferry
ATTN: ELP, R. Maier
ATTN: ELP, G. CHAPMAN
ATTN: ELP, J. Mullis
3 cy ATTN: SUL

DEPARTMENT OF THE AIR FORCE (Continued)

Air Logistics Command
Department of the Air Force
ATTN: MMETH
ATTN: MMEDD

Foreign Technology Division
Air Force Systems Command
ATTN: TQTD, B. Ballard
ATTN: PDJV

Rome Air Development Center
Air Force Systems Command
ATTN: RBRP, C. Lane
ATTN: RBRM, J. Brauer

Rome Air Development Center
Air Force Systems Command
ATTN: ESR, P. Vail
ATTN: ETS, R. Dolan
ATTN: ESER, R. Buchanan
ATTN: ESR, W. Shedd
ATTN: ESE, A Kahan

Space & Missile Systems Organization
Air Force Systems Command
ATTN: AQM
ATTN: AQT, W. Blakney

Space & Missile Systems Organization
Air Force Systems Command
ATTN: DYS

Space & Missile Systems Organization
Air Force Systems Command
ATTN: MNNL
ATTN: MNNH, J. Tucker
ATTN: MNNG

Space & Missile Systems Organization
Air Force Systems Command
ATTN: SZJ, R. Davis

Space & Missile Systems Organization
Air Force Systems Command
ATTN: C. Kelly

Strategic Air Command
Department of the Air Force
ATTN: XPFS, M. Carra

DEPARTMENT OF ENERGY

Department of Energy
Albuquerque Operations Office
ATTN: Document Control for WSSB

DEPARTMENT OF ENERGY CONTRACTORS

Lawrence Livermore Laboratory
ATTN: Document Control for Tech. Info. Dept.

Los Alamos Scientific Laboratory
ATTN: Document Control for J. Freed

Sandia Laboratories
ATTN: Document Control for J. Barnum
ATTN: Document Control for F. Coppage
ATTN: Document Control for J. Hood
ATTN: Document Control for R. Gregory
ATTN: Document Control for W. Dawes

OTHER GOVERNMENT AGENCIES

Central Intelligence Agency
ATTN: OSI/RD

Department of Commerce
National Bureau of Standards
ATTN: Security Officer for J. Mayo-Wells
ATTN: Security Officer for W. Bullis
ATTN: Security Officer for S. Chappell
ATTN: Security Officer for J. French
ATTN: Security Officer for R. Scace
ATTN: Security Officer for J. Humphreys
ATTN: Security Officer for K. Galloway

NASA
Goddard Space Flight Center
ATTN: V. Danchenko
ATTN: J. Adolphsen

NASA
George C. Marshall Space Flight Center
ATTN: M. Nowakowski
ATTN: EGO2
ATTN: H. Yearwood
ATTN: L. Haniter

NASA
ATTN: J. Murphy

NASA
Lewis Research Center
ATTN: M. Baddour

NASA
Ames Research Center
ATTN: G. DeYoung

DEPARTMENT OF DEFENSE CONTRACTORS

Advanced Microdevices, Inc.
ATTN: J. Schlageter

Advanced Research & Applications Corp.
ATTN: R. Armistead

Aerojet Electro-Systems Co.
ATTN: T. Hanscome

Aerospace Corp.
ATTN: S. Bower
ATTN: W. Willis
ATTN: D. Fresh

Aerospace Industries Assoc. of America, Inc.
ATTN: S. Siegel

Battelle Memorial Institute
ATTN: R. Thatcher

BDM Corp.
ATTN: R. Pease
ATTN: D. Alexander
ATTN: D. Wunch

Bendix Corp.
ATTN: E. Meeder

Boeing Co.
ATTN: D. Egelkrout

DEPARTMENT OF DEFENSE CONTRACTORS (Continued)

Boeing Co.
ATTN: A. Johnston
ATTN: I. Arimura
ATTN: W. Rumpza
ATTN: C. Rosenberg

Burr-Brown Research Corp.
ATTN: H. Smith

California Institute of Technology
ATTN: A. Shumka
ATTN: A. Stanley
ATTN: W. Price

Charles Stark Draper Lab., Inc.
ATTN: P. Greiff
ATTN: C. Lai
ATTN: R. Bedingfield
ATTN: A. Schutz
ATTN: R. Ledger

Cincinnati Electronics Corp.
ATTN: L. Hammond
ATTN: C. Stump

Control Data Corp.
ATTN: J. Meehan

University of Denver, Colorado Seminary
ATTN: Security Officer for F. Venditti

E-Systems, Inc.
ATTN: K. Reis

Electronic Industries Association
ATTN: J. Hessman

EMM Corp.
ATTN: F. Krch

Exp. & Math. Physics Consultants
ATTN: T. Jordan

Fairchild Camera and Instrument Corp.
ATTN: Security Control for D. Myers
ATTN: R. Marshall

Ford Aerospace & Communications Corp.
ATTN: J. Davison
ATTN: Technical Information Services

Ford Aerospace & Communications Corp.
ATTN: D. Cadle

Franklin Institute
ATTN: R. Thompson

Garrett Corp.
ATTN: R. Weir

General Dynamics Corp.
ATTN: W. Hansen
ATTN: N. Cohn

General Dynamics Corp.
ATTN: R. Fields
ATTN: O. Wood

DEPARTMENT OF DEFENSE CONTRACTORS (Continued)

General Electric Co.
ATTN: R. Casey
ATTN: L. Sivo
ATTN: J. Peden

General Electric Co.
ATTN: J. Palchefsky, Jr.
ATTN: W. Patterson
ATTN: R. Benedict
ATTN: Technical Library

General Electric Co.
ATTN: J. Reidl

General Electric Co.
ATTN: R. Hellen

General Electric Co.
ATTN: W. Patterson
ATTN: D. Cole
ATTN: J. Gibson

General Electric Co.
ATTN: D. Pepin

General Electric Company—TEMPO
ATTN: M. Espig
ATTN: DASIAC

General Electric Company—TEMPO
ATTN: DASIAC

General Research Corp.
ATTN: Technical Information Office
ATTN: R. Hill

George C. Messenger
ATTN: G. Messenger

Georgia Institute of Technology
ATTN: R. Curry

Georgia Institute of Technology
ATTN: Res & Sec. Coord. for H. Denny

Goodyear Aerospace Corp.
ATTN: Security Control Station

Grumman Aerospace Corp.
ATTN: J. Rogers

GTE Sylvania, Inc.
ATTN: L. Pauples
ATTN: L. Blaisdell
ATTN: C. Thornhill

GTE Sylvania, Inc.
ATTN: H. & V. Group
ATTN: P. Fredrickson
ATTN: H. Ullman
ATTN: J. Waldron

Harris Corp.
ATTN: J. Cornell
ATTN: C. Anderson

Honeywell, Inc.
ATTN: R. Gumm

DEPARTMENT OF DEFENSE CONTRACTORS (Continued)

Honeywell, Inc.
ATTN: C. Cerulli
ATTN: W. Harrison
ATTN: A. Thalheimer

Honeywell, Inc.
ATTN: Technical Library

Honeywell, Inc.
ATTN: K.Gaspard

Hughes Aircraft Co.
ATTN: R. McGowan
ATTN: J. Singletary

Hughes Aircraft Co.
ATTN: E. Smith
ATTN: W. Scott
ATTN: A. Narevsky
ATTN: D. Shumake

IBM Corp.
ATTN: T. Martin
ATTN: H. Mathers
ATTN: F. Tietse

IIT Research Institute
ATTN: I. Mindel

Institute for Defense Analyses
ATTN: Tech. Info. Services

INTEL Corp.
ATTN: M. Jordan

International Business Machine Corp.
ATTN: J. Ziegler

International Tel. & Telegraph Corp.
ATTN: Dept. 608
ATTN: A. Richardson

Intersil Inc.
ATTN: D. MacDonald

IRT Corp.
ATTN: J. Harrity

JAYCOR
ATTN: L. Scott
ATTN: R. Stahl
ATTN: T. Flanagan

Johns Hopkins University
ATTN: P. Partridge

Kaman Sciences Corp.
ATTN: J. Lubell

Litton Systems, Inc.
ATTN: G. Maddox

Lockheed Missiles & Space Co., Inc.
ATTN: M. Smith
ATTN: C. Thompson
ATTN: H. Phillips
ATTN: E. Smith
ATTN: P. Bene

DEPARTMENT OF DEFENSE CONTRACTORS (Continued)

Lockheed Missiles and Space Co., Inc.
ATTN: J. Smith
ATTN: J. Crowley

M.I.T. Lincoln Lab
ATTN: P. McKenzie

Magnavox Govt. & Indus. Electronics Co.
ATTN: W. Richeson

Martin Marietta Corp.
ATTN: W. Brockett
ATTN: W. Janocko
ATTN: H. Cates
ATTN: R. Gaynor

Martin Marietta Corp.
ATTN: E. Carter

McDonnell Douglas Corp.
ATTN: Library
ATTN: D. Dohm
ATTN: M. Stitch

McDonnell Douglas Corp.
ATTN: D. Fitzgerald
ATTN: J. Holmgrem

McDonnell Douglas Corp.
ATTN: Technical Library

Mission Research Corp.
ATTN: Security Officer for C. Longmire

Mission Research Corp.-San Diego
ATTN: J. Raymond
ATTN: J. Azarewicz
ATTN: R. Berger
ATTN: V. Van Lint

Mitre Corp.
ATTN: M. Fitzgerald

Motorola, Inc.
ATTN: A. Christensen

Motorola, Inc.
ATTN: L. Clark

National Academy of Sciences
ATTN: R. Shane

National Semiconductor Corp.
ATTN: R. Wang
ATTN: A. London

University of New Mexico
ATTN: H. Southward

Northrop Corp.
ATTN: T. Jackson
ATTN: J. Srour
ATTN: P. Eisenberg

Northrop Corp.
ATTN: D. Strobel
ATTN: L. Apodaca
ATTN: P. Gardner

DEPARTMENT OF DEFENSE CONTRACTORS (Continued)

Physics International Co.
ATTN: J. Shea
ATTN: Division 6000
ATTN: J. Huntington

R&D Associates
ATTN: C. MacDonald
ATTN: R. Poll
ATTN: S. Rogers

Rand Corp.
ATTN: C. Crain

Raytheon Co.
ATTN: J. Ciccio

Raytheon Co.
ATTN: A. Van Doren
ATTN: H. Flescher

RCA Corp.
ATTN: V. Mancino
ATTN: G. Brucker

RCA Corp.
ATTN: D. O'Connor
ATTN: Office N103

RCA Corp.
ATTN: R. Killion

RCA Corp.
ATTN: E. Van Keuren
ATTN: J. Saultz

RCA Corp.
ATTN: W. Allen

Rensselaer Polytechnic Institute
ATTN: R. Gutmann

Research Triangle Institute
ATTN: M. Simons, Jr.

Rockwell International Corp.
ATTN: V. DeMartino
ATTN: T. Oki
ATTN: G. Messenger
ATTN: V. Strahan
ATTN: J. Dell

Rockwell International Corp.
ATTN: G. Stevens

Rockwell International Corp.
ATTN: TIC BA09
ATTN: T. Yates

Sanders Associates, Inc.
ATTN: L. Brodeur

Science Applications, Inc.
ATTN: D. Long
ATTN: J. Naber
ATTN: V. Verbinski
ATTN: V. Ophan

Science Applications, Inc.
ATTN: W. Chadsey

DEPARTMENT OF DEFENSE CONTRACTORS (Continued)

Science Applications, Inc.
ATTN: D. Stribling

Singer Co.
ATTN: J. Brinkman

Singer Co.
ATTN: R. Spiegel

Solar Energy Research Institute
ATTN: A. Stanley

Sperry Rand Corp.
ATTN: Engineering Laboratory

Sperry Rand Corp
ATTN: F. Scaravaglione
ATTN: P. Maraffino
ATTN: C. Craig
ATTN: R. Viola

Sperry Rand Corp.
ATTN: D. Schow

Sperry Univac
ATTN: J. Inda

Spire Corp.
ATTN: R. Little

SRI International
ATTN: A. Whitson
ATTN: P. Dolan

Systron-Donner Corp.
ATTN: J. Indelicato

DEPARTMENT OF DEFENSE CONTRACTORS (Continued)

Teledyne Ryan Aeronautical
ATTN: J. Rawlings

Texas Instruments, Inc.
ATTN: R. Stehlin
ATTN: A. Peletier

TRW Defense & Space Sys. Group
ATTN: A. Pavelko
ATTN: R. Kingsland
ATTN: P. Guilfoyle
ATTN: O. Adams
ATTN: A. Witteles
ATTN: N. Holloway

TRW Defense & Space Sys. Group
ATTN: F. Fay
ATTN: M. Gorman
ATTN: R. Kirtes

TRW Systems and Energy
ATTN: D. Millward
ATTN: B. Gililland

Vought Corp.
ATTN: Technical Data Center
ATTN: R. Tomme
ATTN: Library

Westinghouse Electric Co.
ATTN: L. McPherson

Westinghouse Electric Corp.
ATTN: H. Kalapaca
ATTN: D. Crichi